Measurement of Properties of the Higgs boson in bosonic channels using the ATLAS detector (including rare decays)

Tomoe Kishimoto[1] on behalf of the ATLAS collaboration

[1]Kobe University

August 26 2013

Outline

- Motivation & overview
- Measurement of Higgs mass
  - $H \to \gamma\gamma$, $H \to ZZ^* \to 4l$
- Measurement of signal strength of production and decay
  - $H \to \gamma\gamma$, $H \to ZZ^* \to 4l$, $H \to WW^* \to l\nu l\nu$, $(H \to Z\gamma)$
- Spin/CP (J^P) discrimination
  - $H \to \gamma\gamma$, $H \to ZZ^* \to 4l$, $H \to WW^* \to l\nu l\nu$
- Summary

- Combined measurements:
  - "Combination of the Higgs Boson Main Properties Measurements using the ATLAS detector" , Andrea Gabrielli

Motivation & overview

- We have found a Higgs boson
- It is important to measure its properties:
  - mass, signal strengths, spin-parity
  - Is it really the SM Higgs boson?
- This talk focuses on bosonic decay channels ($\gamma\gamma$, ZZ^*, WW^*, $Z\gamma$)
- Following results are based on full 2011+2012 dataset
- 20.7fb^{-1} at 8 TeV, 4.8 fb^{-1} at 7 TeV

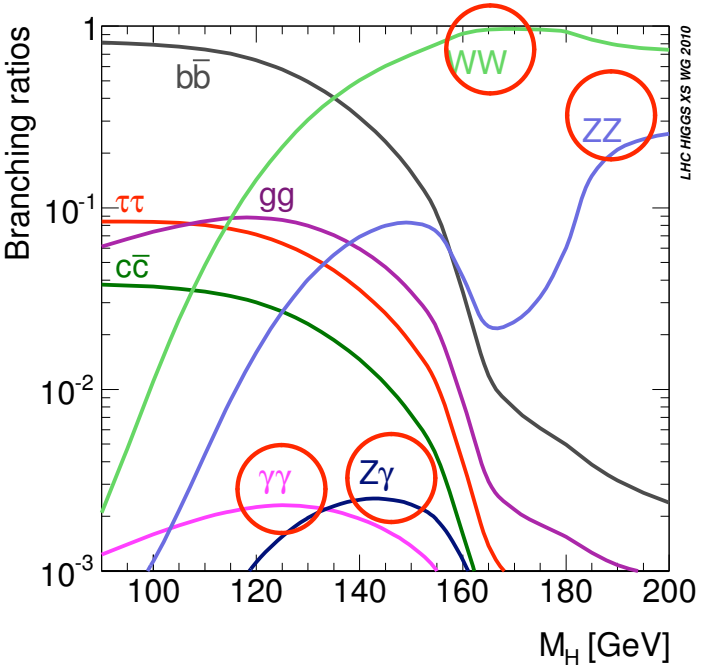

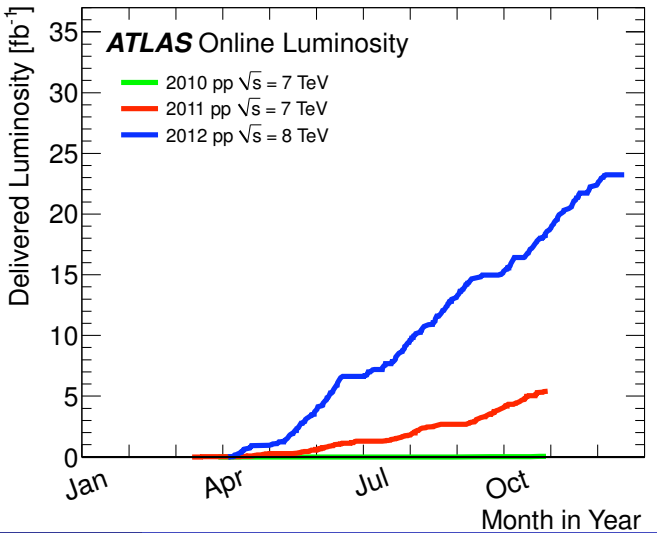

Measurement of Higgs mass

ATLAS-CONF-2013-012

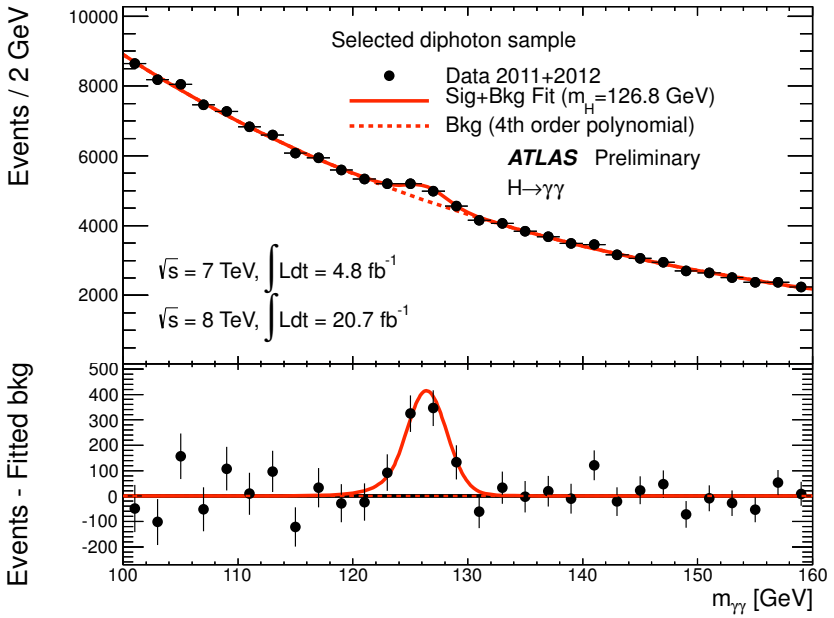

ATLAS-CONF-2013-013

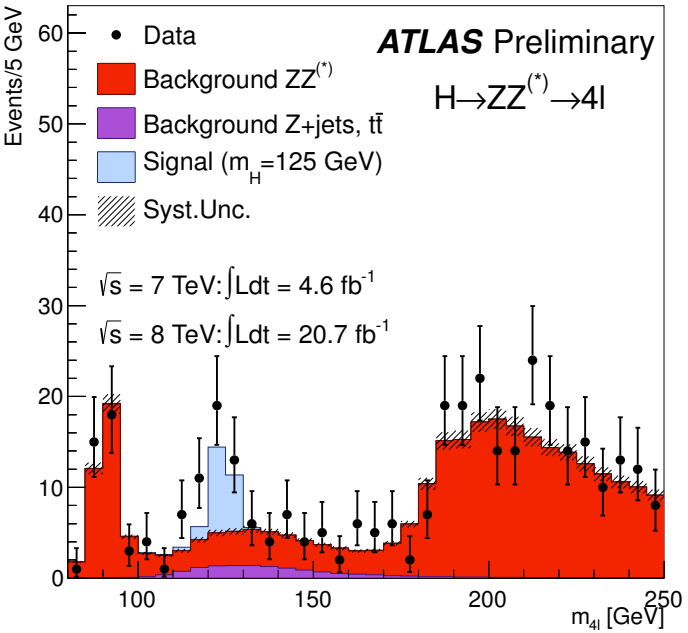

- High resolution mass measurements from H$\longrightarrow \gamma\gamma$ and H$\longrightarrow$ ZZ* $\longrightarrow$ 4l
- Clear peaks in $m_{\gamma\gamma}$ and m_{4l} distributions

Measurement of Higgs mass

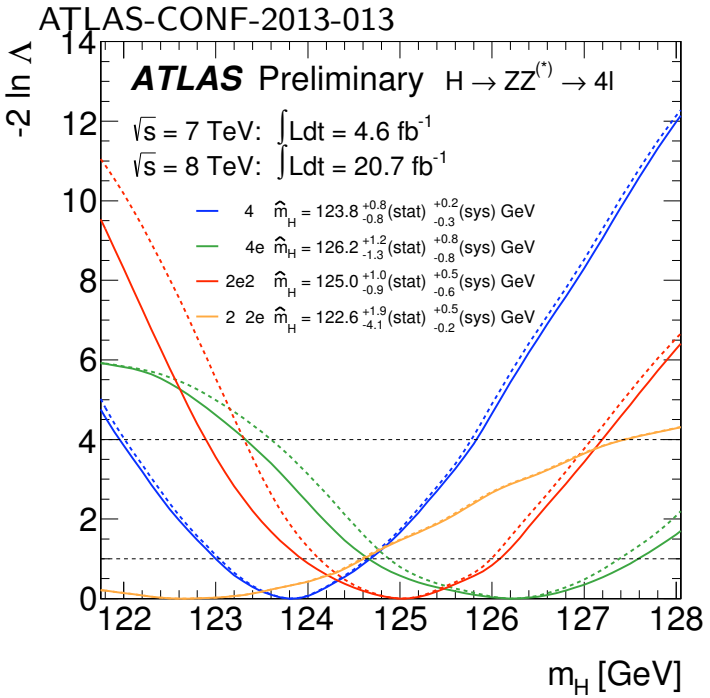

- Mass is extracted from profile likelihood fit to data

$$-2ln\Lambda = -2ln\frac{L(m_H,\hat{\hat{\theta}}(m_H))}{L(\hat{m_H},\hat{\theta})}$$

- Signal strength $\mu(=\sigma/\sigma_{SM})$ is a free parameter

- Best-fit mass:

$H\to\gamma\gamma$: **126.8 $\pm$0.2(stat) $\pm$0.7(syst) GeV**

$H\to ZZ^*\to 4l$: **124.3$^{+0.6}_{-0.5}$(stat) $^{+0.5}_{-0.3}$(syst) GeV**

Measurement of signal strength: Higgs production at LHC

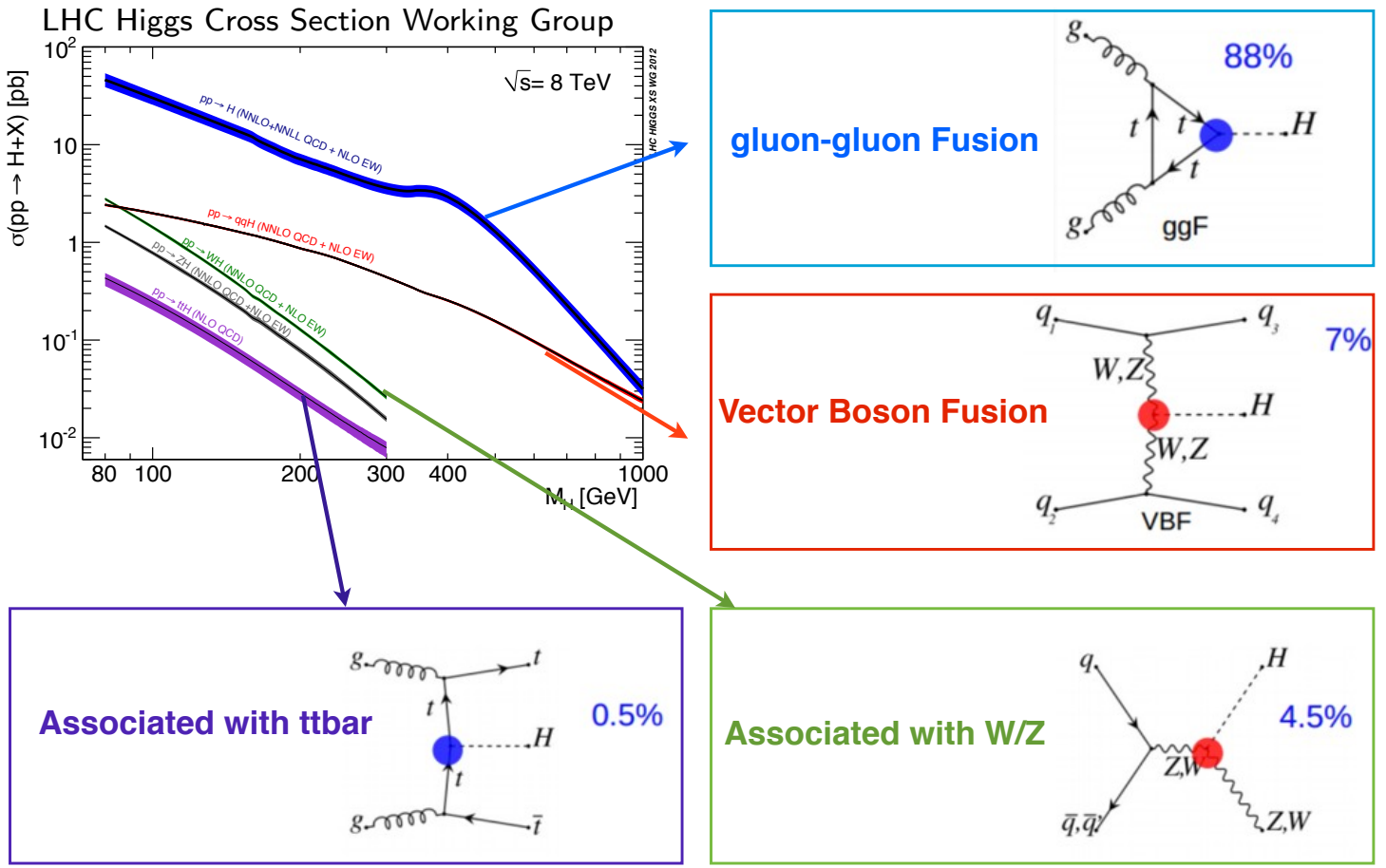

- Signal strengths in different production processes and the ratio (e.g $\mu_{ggH+ttH}/\mu_{VBF+VH}$) are also measured

Measurement of signal strength: H$\to \gamma\gamma$

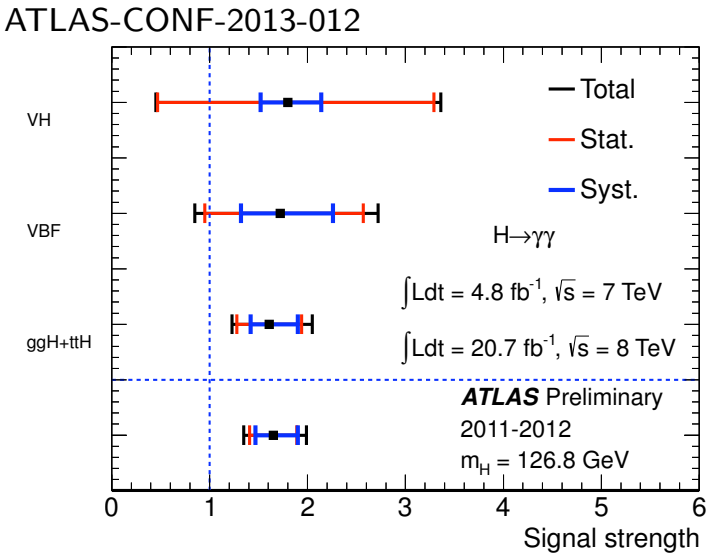

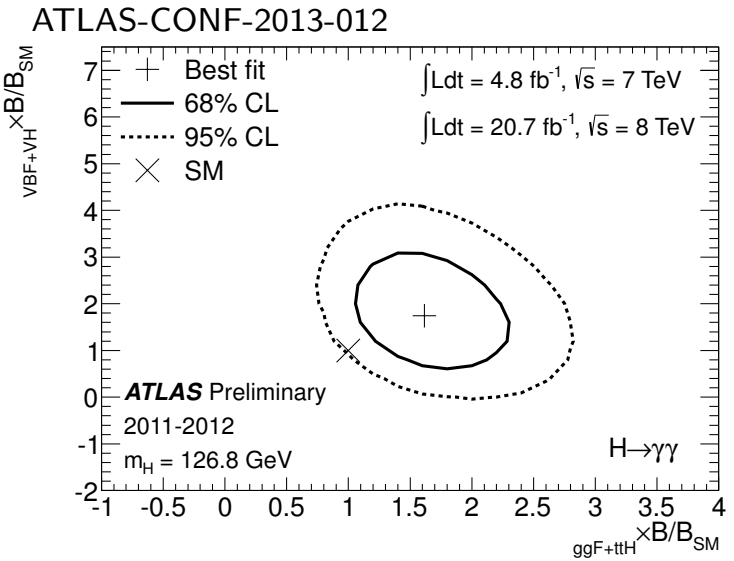

- Overall signal strength $\mu(=\sigma/\sigma_{SM})$ at 126.8 GeV:

$$\mathbf{1.65 \pm 0.24(stat)\ ^{+0.25}_{-0.18}(syst)}$$

- Signal strengths tend to be high in all production modes
- Compatibility with SM expectation: 2.3σ

Measurement of signal strength: H→ZZ* →4l

- Overall signal strength μ at 124.3 GeV: $\mathbf{1.7}^{+0.5}_{-0.4}$
- Signal strength by production mode:

	$\mu_{ggF+ttH} \times B/B_{SM}$	$\mu_{VBF+VH} \times B/B_{SM}$	Ratio
Measured value	$1.8^{+0.8}_{-0.5}$	$1.2^{+3.8}_{-1.4}$	$0.7^{+2.4}_{-0.3}$

- Signal strengths are consistent with 1 within 2σ uncertainties

ATLAS-CONF-2013-013

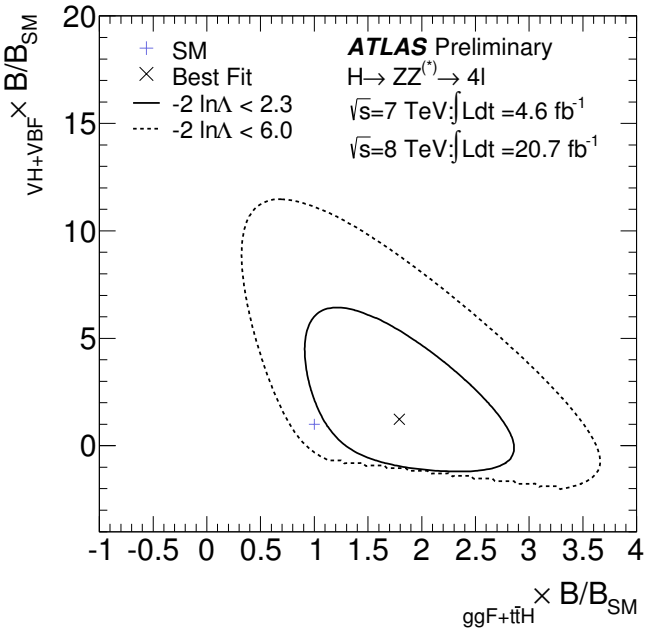

ATLAS-CONF-2013-013

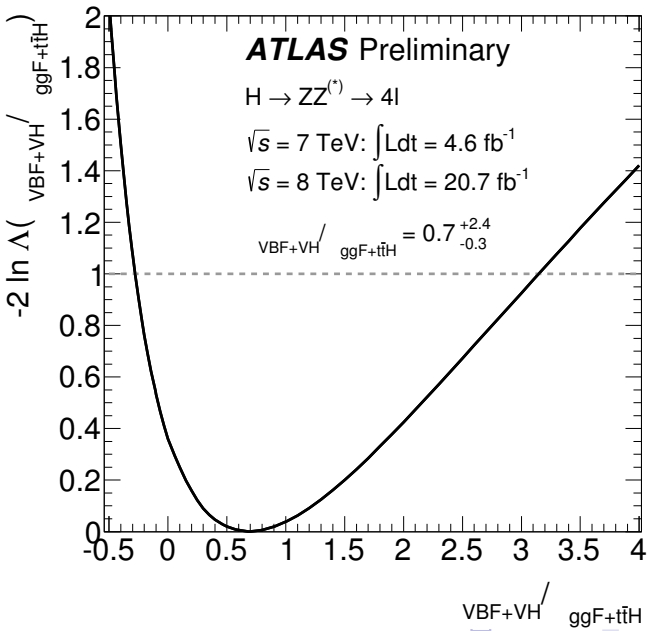

Measurement of signal strength: H→WW* →lνlν

- Overall signal strength μ at 125 GeV:

$1.01 \pm 0.21(\text{stat}) \pm 0.19(\text{theo.syst}) \pm 0.12(\text{expt.syst}) \pm 0.04(\text{lumi})$

- Signal strength by production mode:

	$\mu_{ggF} \times B/B_{SM}$	$\mu_{VBF+VH} \times B/B_{SM}$
Measured value	$0.82 \pm 0.24(\text{stat.}) \pm 0.28(\text{syst})$	$1.66 \pm 0.67(\text{stat.}) \pm 0.42(\text{syst})$

- All values are consistent with 1(= the SM expectation)

ATLAS-CONF-2013-030

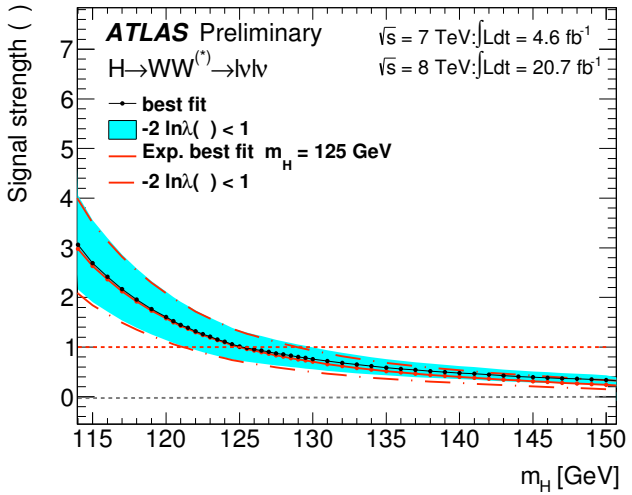

ATLAS-CONF-2013-030

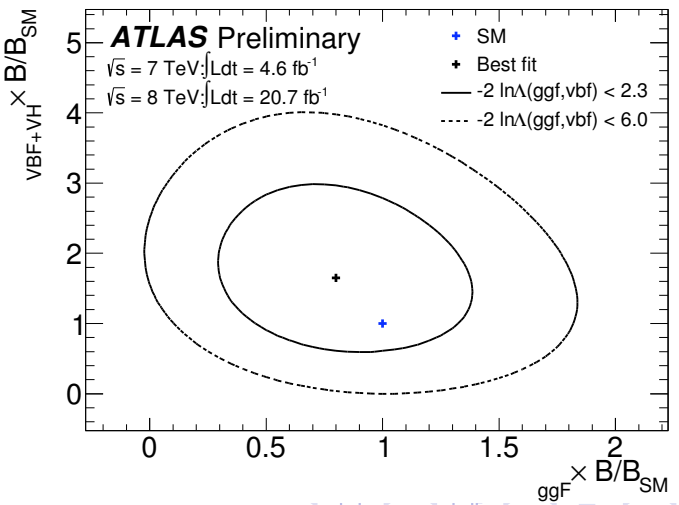

Search for the Higgs in $Z\gamma$ decay mode

- The yield of $H \to Z\gamma \to ll\gamma$ is similar to $H \to ZZ^* \to 4l$, but larger backgrounds
- Limits are extracted from $\Delta m = m_{ll\gamma} - m_{ll}$
  - Insensitive to the contribution to the signal from FSR in $H \to \mu\mu$

ATLAS-CONF-2013-009

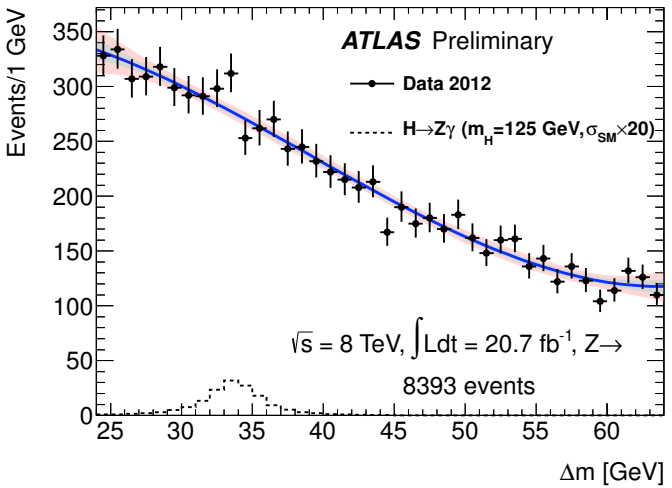

ATLAS-CONF-2013-009

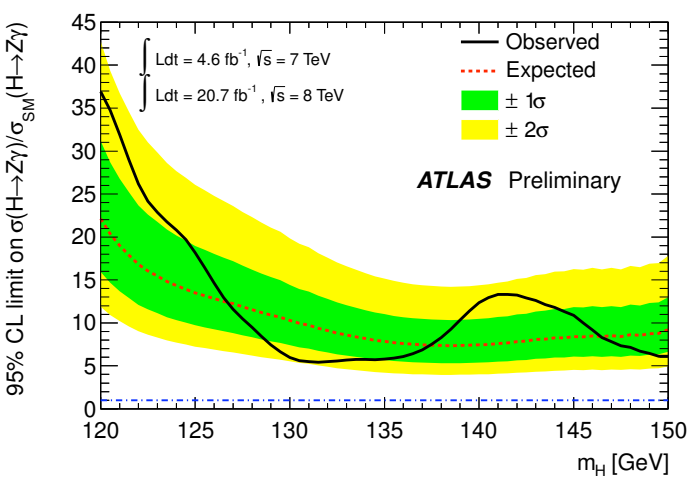

- Observed(expected) upper limit at 125 GeV: **18.2×SM(13.5×SM)**

Spin/CP discrimination: H→ZZ* →4l

- Sensitive through many angular variables $(\theta^*, \phi_1, \phi, \theta_1, \theta_2)$ + Z masses
- Several J^P hypotheses are tested against the $J^P=0^P$ hypothesis (=Standard Model Higgs) with Boosted Decision Tree

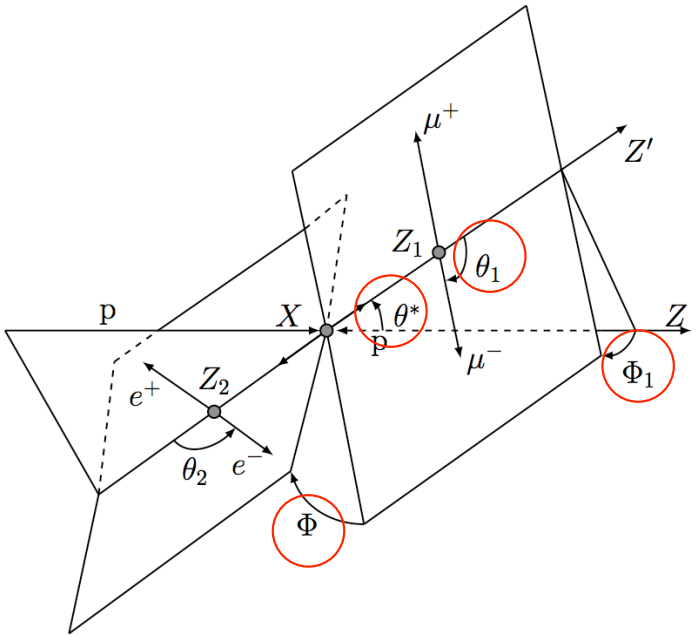

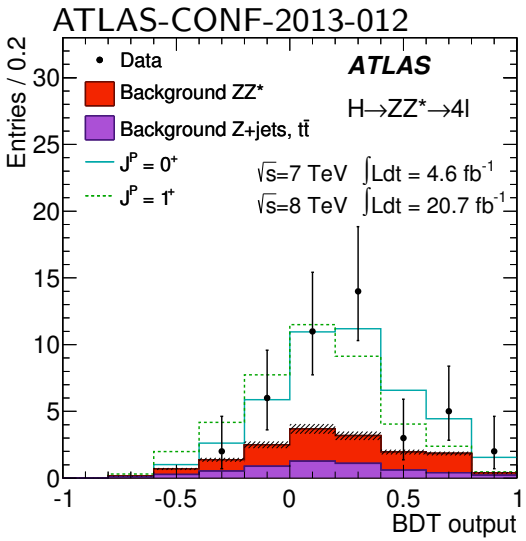

J^P	0^-	1^+	1^-	2^+_m
BDT 1-CL$_s$	97.8%	99.8%	94.0%	83.1%

1-CL$_s$: X% level preference for he SM 0^+

2^+_m: minimal graviton-like spin-2 model

- Data strongly favor $J^P = 0^+$

Spin/CP discrimination: H→ $\gamma\gamma$ and H→WW* →lvlv

- H→ $\gamma\gamma$ strongly disfavors spin 1 (Yang-Landau theorem)
- Minimal graviton-like spin-2 model(2^+_m) hypothesis is tested against the SM(0^+) hypothesis. Varied qqbar→X and gg→X fractions
- $\gamma\gamma$: Sensitive through $\cos\theta^*$ = angular distribution of photons in the resonance rest frame
- WW*: Sensitive through kinematic variables(m_{ll}, $p_{T,ll}$, $\Delta\Phi_{ll}$, m_T)

arXiv:1307.1432

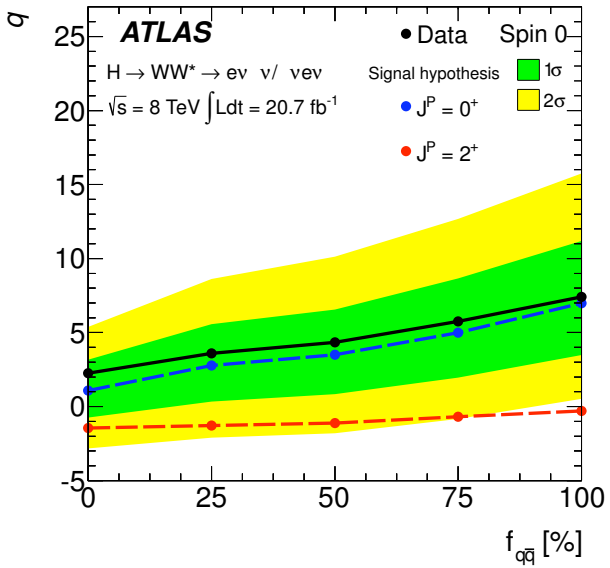

f_{qqbar}	0%	25%	50%	75%	100%
$\gamma\gamma$ 1-CL$_s$	99.3%	94.6%	74%	66.3%	87.6%
WW 1-CL$_s$	95.2%	98.0%	99.2%	99.7%	99.9%

- WW 1-CLs: $J^P(1^+)$ 92.0%, $J^P(1^-)$ 98.3%
- In both channels, data agree closely with SM(0^+) hypothesis

Summary

- Measurement of properties of the Higgs boson in ATLAS using 2011+2012 dataset presented
- Its mass is determined with $<$1 GeV uncertainty:
  - $\gamma\gamma$: 126.8 $\pm$0.2(stat) $\pm$0.7(syst) GeV
  - ZZ^*: 124.3 $^{+0.6}_{-0.5}$(stat) $^{+0.5}_{-0.3}$(syst) GeV
- Its signal strengths, spin and parity are almost consistent with those of Standard Model Higgs boson
  - $\gamma\gamma$: μ =1.65 $\pm$0.24(stat) $^{+0.25}_{-0.18}$(syst)
  - ZZ^*: μ =1.7 $^{+0.5}_{-0.4}$
  - WW^*: μ =1.01$\pm$0.21(stat)$\pm$0.19(theo.syst)$\pm$0.12(expt.syst)$\pm$0.04(lumi)

Backup

2^+_m model

$$A(X \to VV) = \Lambda^{-1} \left[2g_1^{(2)} t_{\mu\nu} f^{*1,\mu\alpha} f^{*2,\nu\alpha} + 2g_2^{(2)} t_{\mu\nu} \frac{q_\alpha q_\beta}{\Lambda^2} f^{*1,\mu\alpha} f^{*2,\nu,\beta} \right.$$
$$+ g_3^{(2)} \frac{\tilde{q}^\beta \tilde{q}^\alpha}{\Lambda^2} t_{\beta\nu} (f^{*1,\mu\nu} f^{*2}_{\mu\alpha} + f^{*2,\mu\nu} f^{*1}_{\mu\alpha}) + g_4^{(2)} \frac{\tilde{q}^\nu \tilde{q}^\mu}{\Lambda^2} t_{\mu\nu} f^{*1,\alpha\beta} f^{*(2)}_{\alpha\beta}$$
$$+ m_V^2 \left(2g_5^{(2)} t_{\mu\nu} \epsilon_1^{*\mu} \epsilon_2^{*\nu} + 2g_6^{(2)} \frac{\tilde{q}^\mu q_\alpha}{\Lambda^2} t_{\mu\nu} (\epsilon_1^{*\nu} \epsilon_2^{*\alpha} - \epsilon_1^{*\alpha} \epsilon_2^{*\nu}) + g_7^{(2)} \frac{\tilde{q}^\mu \tilde{q}^\nu}{\Lambda^2} t_{\mu\nu} \epsilon_1^* \epsilon_2^* \right)$$
$$\left. + g_8^{(2)} \frac{\tilde{q}_\mu \tilde{q}_\nu}{\Lambda^2} t_{\mu\nu} f^{*1,\alpha\beta} \tilde{f}^{*(2)}_{\alpha\beta} + g_9^{(2)} t_{\mu\alpha} \tilde{q}^\alpha \epsilon_{\mu\nu\rho\sigma} \epsilon_1^{*\nu} \epsilon_2^{*\rho} q^\sigma + \frac{g_{10}^{(2)} t_{\mu\alpha} \tilde{q}^\alpha}{\Lambda^2} \epsilon_{\mu\nu\rho\sigma} q^\rho \tilde{q}^\sigma \left(\epsilon_1^{*\nu} (q\epsilon_2^*) + \epsilon_2^{*\nu} (q\epsilon_1^*) \right) \right] .$$

scenario (J^P)	$X \to ZZ$ decay parameters	X production parameters	comments
0^+	$a_1 \neq 0$ in Eq. (2)	$gg \to X$	SM Higgs-like scalar
0^-	$a_3 \neq 0$ in Eq. (2)	$gg \to X$	pseudo-scalar
1^+	$g_{12} \neq 0$ in Eq. (4)	$q\bar{q} \to X$: ρ_{11}, $\rho_{12} \neq 0$ in Eq. (9)	exotic pseudo-vector
1^-	$g_{11} \neq 0$ in Eq. (4)	$q\bar{q} \to X$: ρ_{11}, $\rho_{12} \neq 0$ in Eq. (9)	exotic vector
2^+_m	$g_1^{(2)} = g_5^{(2)} \neq 0$ in Eq. (5)	$gg \to X$: $g_1^{(2)} \neq 0$ in Eq. (5) $q\bar{q} \to X$: $\rho_{21} \neq 0$ in Eq. (10)	Graviton-like tensor with minimal couplings
2^+_L	$c_2 \neq 0$ in Eq. (6)	$gg \to X$: $g_2^{(2)} = g_3^{(2)} \neq 0$ in Eq. (5) $q\bar{q} \to X$: ρ_{21}, $\rho_{22} \neq 0$ in Eq. (10)	Graviton-like tensor longitudinally polarized and with $J_z = 0$ contribution
2^-	$g_8^{(2)} = g_9^{(2)} \neq 0$ in Eq. (5)	$gg \to X$: $g_1^{(2)} \neq 0$ in Eq. (5) $q\bar{q} \to X$: ρ_{21}, $\rho_{22} \neq 0$ in Eq. (10)	"pseudo-tensor"

- g_1(in production and decay) and g_5(in decay) set to 1 for 2^+_m and couplings g_1(in production), and g_8 and g_9(in decay) set to 1 for 2^-

Spin analysis: statistical treatment

- Likelihood $L(\epsilon, \theta)$ constructed with one parameter of interest ϵ, which represents the fraction of 0^+ signal events in the total signal expectation

$$L(\epsilon, \mu, \theta) = \prod_i^{N_{bins}} P(N_i|\mu(\epsilon S_{0^+,i}(\vec{\theta}) + (1-\epsilon)S_{2^+,i}(\vec{\theta})) + b_i(\vec{\theta})) \times \prod_j^{N_{sys}} A(\tilde{\theta}_j|\theta_j)$$

- The test statistic q is defined as a ratio of likelihoods:

$$q = log\frac{L(H_{0^+})}{L(H_{2^+_m})} = log\frac{L(\epsilon{=}1,\hat{\hat{\mu}}_{\epsilon=1},\hat{\hat{\theta}}_{\epsilon=1})}{L(\epsilon{=}0,\hat{\hat{\mu}}_{\epsilon=0},\hat{\hat{\theta}}_{\epsilon=0})}$$

- Distributions of test statistic obtained using toy MC

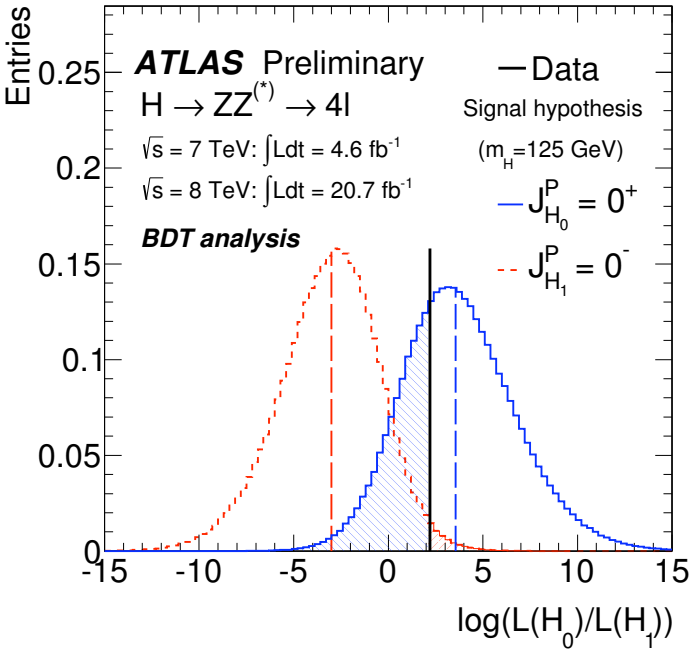

H $\rightarrow \gamma\gamma$: selections

- Photons:
  - $E_T > 40$, 30 GeV. $|\eta| < 2.37$(excluding $1.37 < |\eta| < 1.56$)
  - Track isolation: p_T sum of all tracks with $p_T > 1$ GeV in a cone of $\Delta R < 0.2$ around each photon. Required to be below 2.6 GeV
  - Calorimeter isolation: transverse energy sum (of topological cluster) deposited in the calorimeter around the photon in a cone of $\Delta R = 0.4$. Required to be below 6 GeV
  - Requirements on EM shower shape variables:

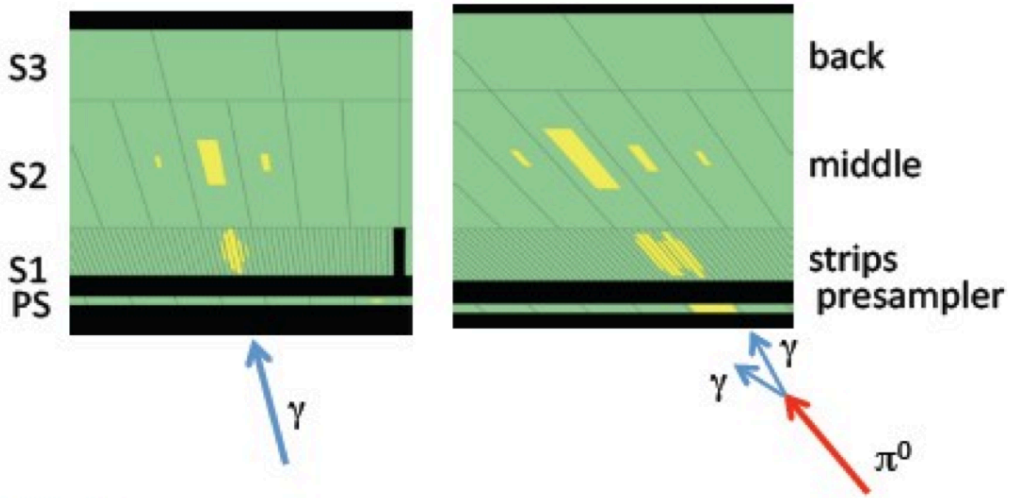

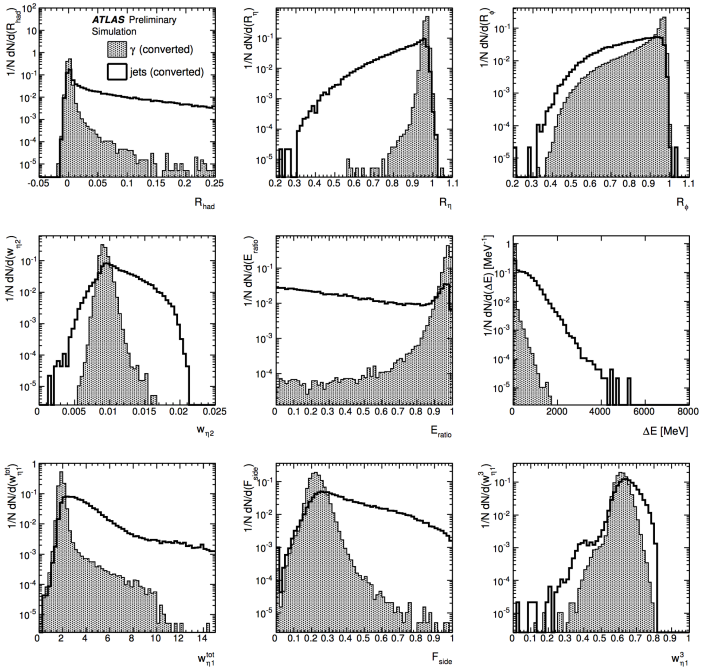

$H \to \gamma\gamma$: categorization

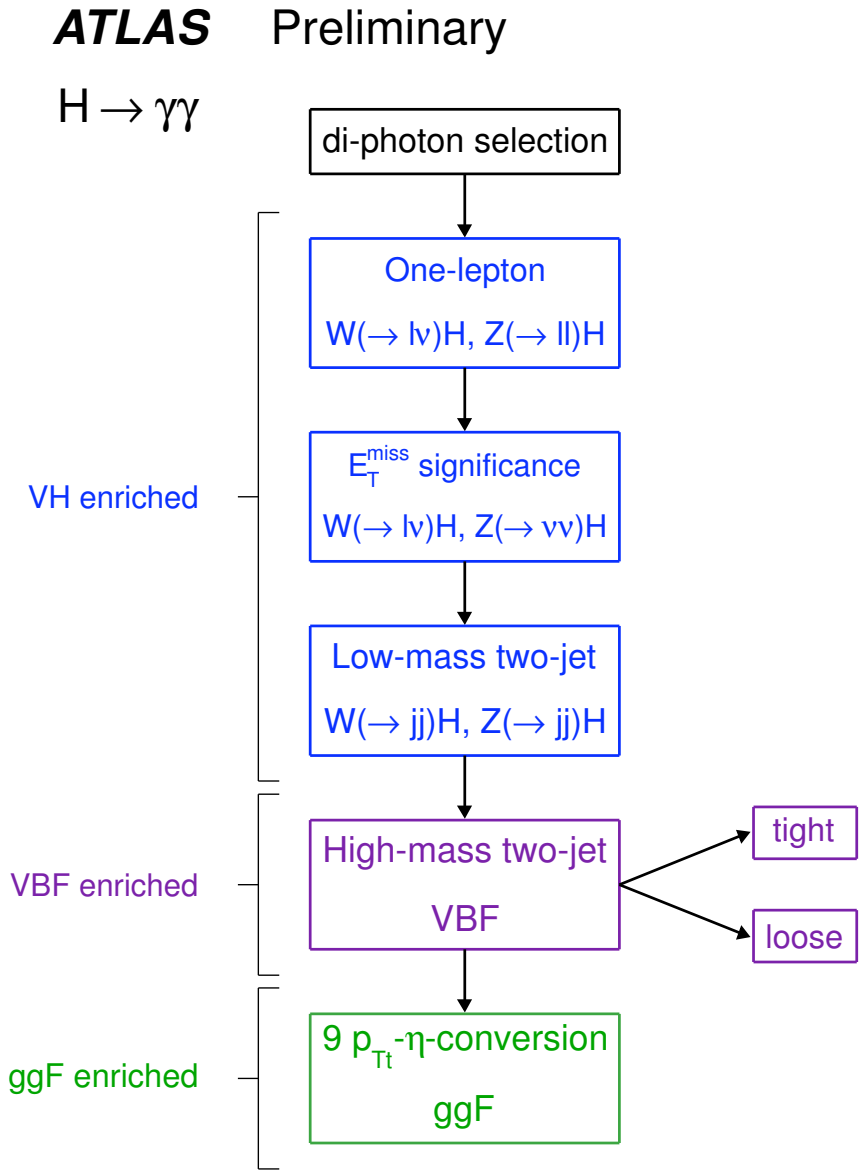

- $p_{Tt} = |\vec{p_T}^{\gamma\gamma} \times \hat{t}|$,
  where $\hat{t} = \frac{\vec{p_T}^{\gamma 1} - \vec{p_T}^{\gamma 2}}{|\vec{p_T}^{\gamma 1} - \vec{p_T}^{\gamma 2}|}$

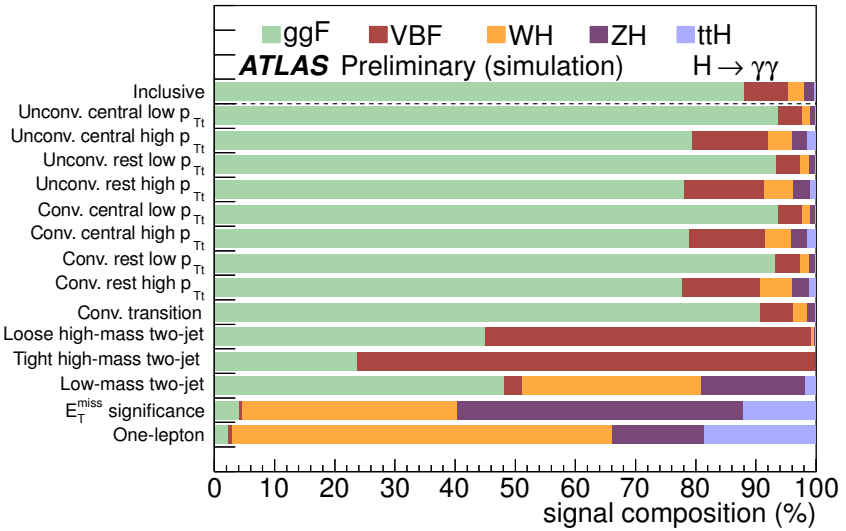

H → γγ: VBF category

- Eight discriminating variables are used to build a boosted decision tree
- m_{jj}, η_{j1}, η_{j2}, $\Delta\eta_{jj}$, p_{Tt}, $\Delta\Phi_{\gamma\gamma;jj}$, $\eta^* = \eta_{\gamma\gamma} - \frac{\eta_{j1}-\eta_{j2}}{2}$, $\Delta R^{\gamma j}_{min}$

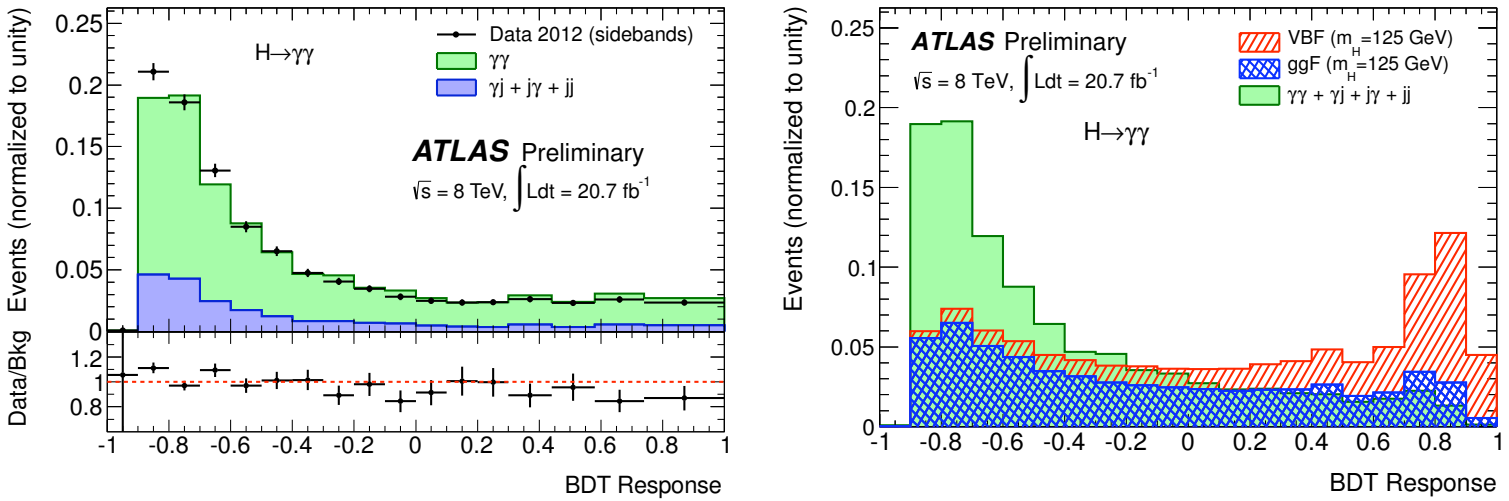

- BDT $> 0.74 \rightarrow$ tight, $0.44 <$ BDT $< 0.74 \rightarrow$ loose

$H \to \gamma\gamma$: number of signals and signal mass resolution

$\sqrt{s}$	8 TeV						
Category	N_D	N_S	$gg \to H$ [%]	VBF [%]	WH [%]	ZH [%]	ttH [%]
Unconv. central, low p_{Tt}	10900	51.8	93.7	4.0	1.4	0.8	0.2
Unconv. central, high p_{Tt}	553	7.9	79.3	12.6	4.1	2.5	1.4
Unconv. rest, low p_{Tt}	41236	107.9	93.2	4.0	1.6	1.0	0.1
Unconv. rest, high p_{Tt}	2558	16.0	78.1	13.3	4.7	2.8	1.1
Conv. central, low p_{Tt}	7109	33.1	93.6	4.0	1.3	0.9	0.2
Conv. central, high p_{Tt}	363	5.1	78.9	12.6	4.3	2.7	1.5
Conv. rest, low p_{Tt}	38156	97.8	93.2	4.1	1.6	1.0	0.1
Conv. rest, high p_{Tt}	2360	14.4	77.7	13.0	5.2	3.0	1.1
Conv. transition	14864	40.1	90.7	5.5	2.2	1.3	0.2
Loose high-mass two-jet	276	5.3	45.0	54.1	0.5	0.3	0.1
Tight high-mass two-jet	136	8.1	23.8	76.0	0.1	0.1	0.0
Low-mass two-jet	210	3.3	48.1	3.0	29.7	17.2	1.9
E_T^{miss} significance	49	1.3	4.1	0.5	35.7	47.6	12.1
One-lepton	123	2.9	2.2	0.6	63.2	15.4	18.6
All categories (inclusive)	118893	395.0	88.0	7.3	2.7	1.5	0.5

$\sqrt{s}$	8 TeV				
Category	σ_{CB}(GeV)	Observed	N_S	N_B	N_S/N_B
Unconv. central, low p_{Tt}	1.50	911	46.6	881	0.05
Unconv. central, high p_{Tt}	1.40	49	7.1	44	0.16
Unconv. rest, low p_{Tt}	1.74	4611	97.1	4347	0.02
Unconv. rest, high p_{Tt}	1.69	292	14.4	247	0.06
Conv. central, low p_{Tt}	1.68	722	29.8	687	0.04
Conv. central, high p_{Tt}	1.54	39	4.6	31	0.15
Conv. rest, low p_{Tt}	2.01	4865	88.0	4657	0.02
Conv. rest, high p_{Tt}	1.87	276	12.9	266	0.05
Conv. transition	2.52	2554	36.1	2499	0.01
Loose High-mass two-jet	1.71	40	4.8	28	0.17
Tight High-mass two-jet	1.64	24	7.3	13	0.57
Low-mass two-jet	1.62	21	3.0	21	0.14
E_T^{miss} significance	1.74	8	1.1	4	0.24
One-lepton	1.75	19	2.6	12	0.20
Inclusive	1.77	14025	355.5	13280	0.03

- The total efficiency for the signal selection is expected to be 37.5%
- The resolution of the reconstructed diphoton mass is dominated by the photon energy resolution

$H \to \gamma\gamma$: backdounds

- Two-dimensional sideband method to estimate the relative $Z+\gamma$ and Z+jets fractions

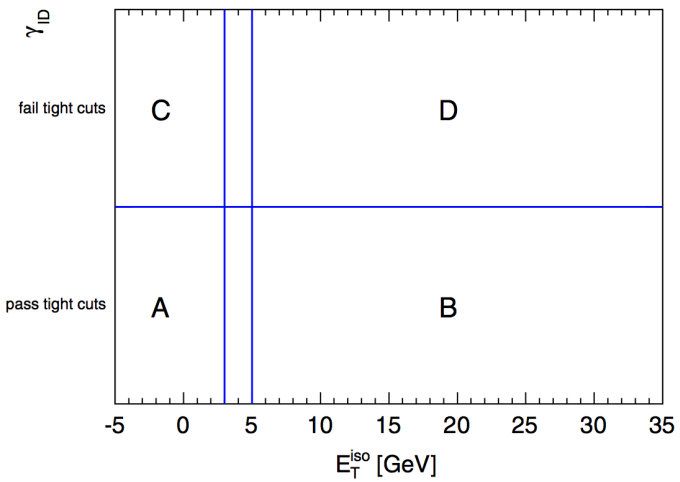

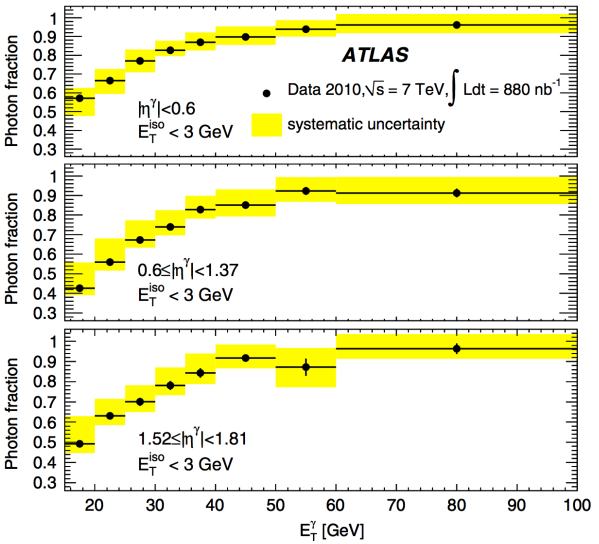

- $N_A^{sig} = N_A - (N_B - c_B N_A^{sig}) \frac{N_C - c_C N_A^{sig}}{N_D - c_D N_A^{sig}}$

$H \longrightarrow \gamma\gamma$: backdounds

- Data-driven background decomposition

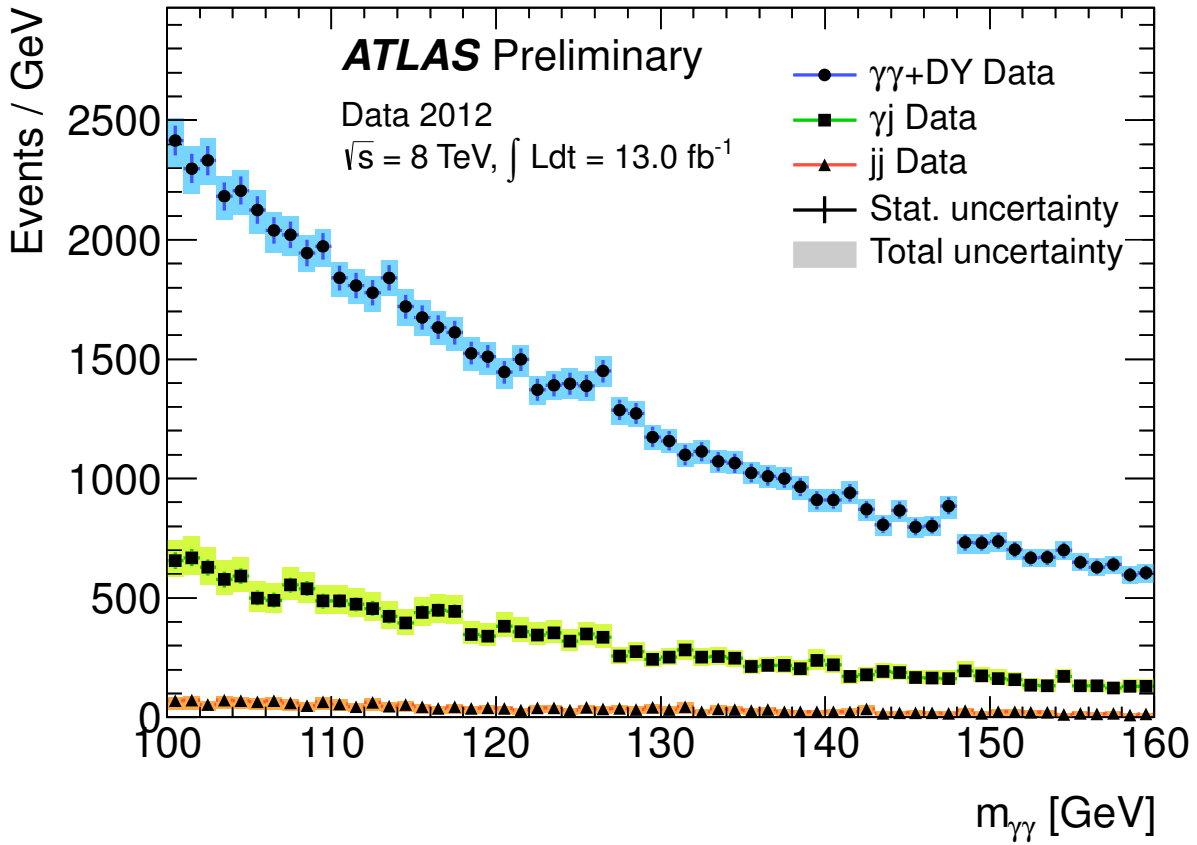

H $\rightarrow \gamma\gamma$: systematic uncertainties

Table 5: Summary of the impact of systematic uncertainties on the signal yields for the analysis of the 8 TeV data.

Systematic uncertainties	Value(%)			Constraint
Luminosity	±3.6			
Trigger	±0.5			
Photon Identification	±2.4			Log-normal
Isolation	±1.0			
Photon Energy Scale	±0.25			
Branching ratio	±5.9% – ±2.1% (m_H = 110 - 150 GeV)			Asymmetric Log-normal
Scale	ggF: $^{+7.2}_{-7.8}$	VBF: $^{+0.2}_{-0.2}$	WH: $^{+0.2}_{-0.6}$	Asymmetric
	ZH: $^{+1.6}_{-1.5}$	ttH: $^{+3.8}_{-9.3}$		Log-normal
PDF+α_s	ggF: $^{+7.5}_{-6.9}$	VBF: $^{+2.6}_{-2.7}$	WH: ±3.5	Asymmetric
	ZH: ±3.6	ttH: ±7.8		Log-normal
Theory cross section on ggF	Tight high-mass two-jet:		±48	Log-normal
	Loose high-mass two-jet:		±28	
	Low-mass two-jet:		±30	

- **Mass uncertainties**
- Uncertainties arise from the extrapolation of the photon energy scale from the Z $\rightarrow$ ee electron energy scale (0.3%), the material modelling (0.3%) and the presampler energy scale (0.1%).

$H \to \gamma\gamma$: results

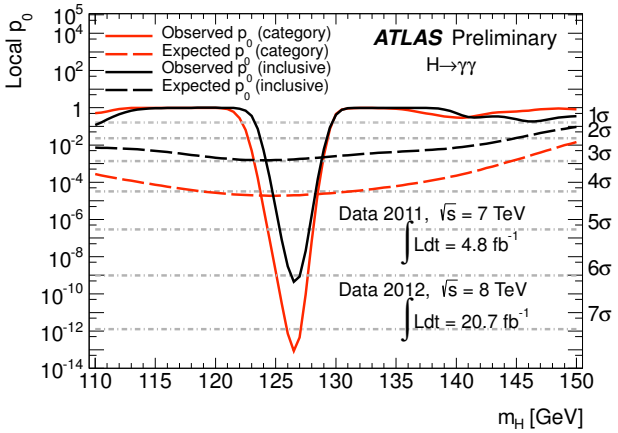

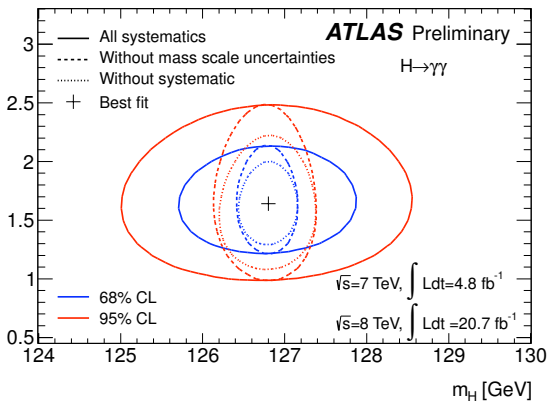

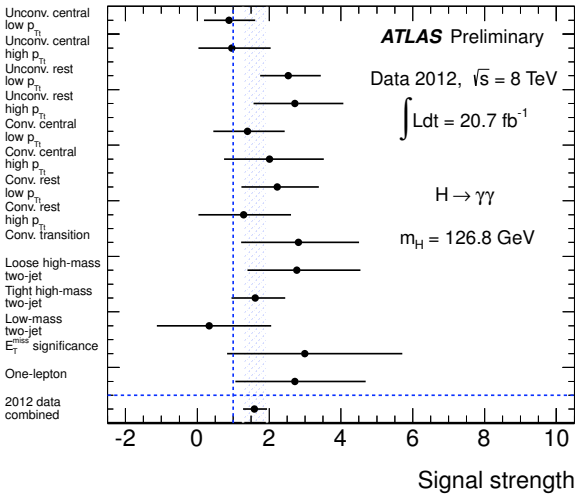

$H \to \gamma\gamma$: spin

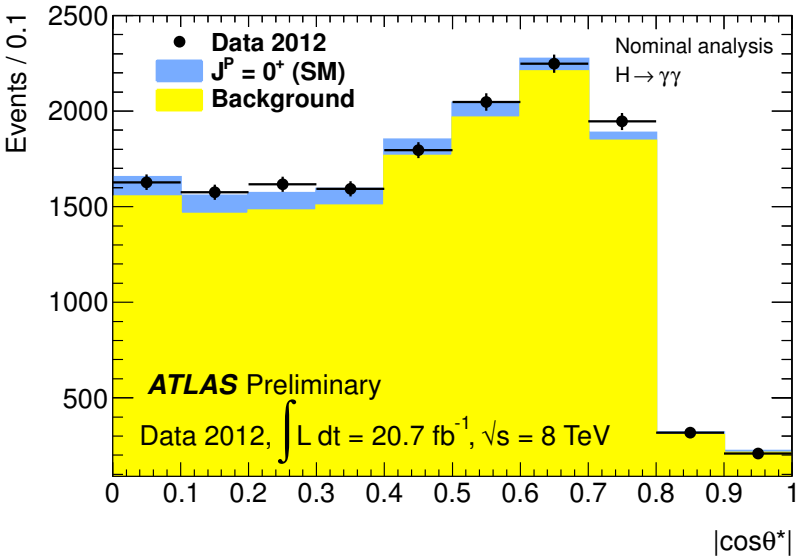

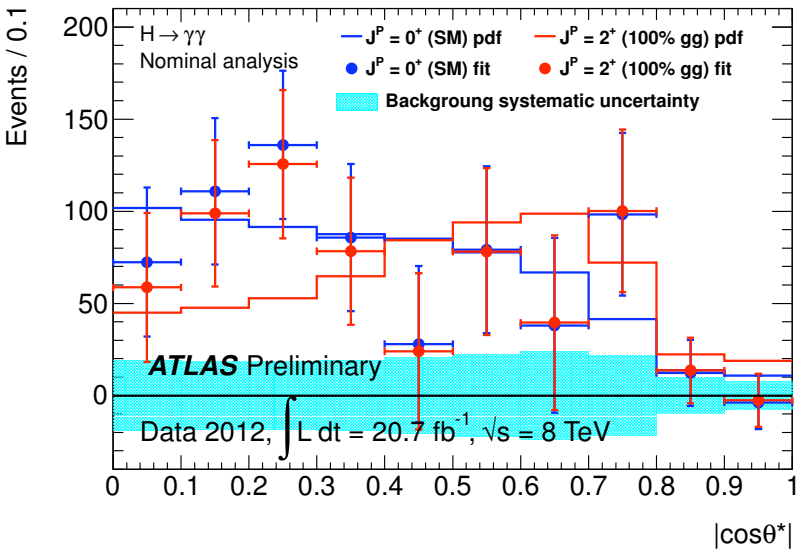

- Right plot shows distributions of background-subtracted data in the signal region as a function of $|\cos\theta^*|$. The two sets of points correspond to the subtraction of the different profiled background shapes in the case of the conditional spin-0 and spin-2 fits

H $\rightarrow$ZZ* $\rightarrow$ 4l: selections

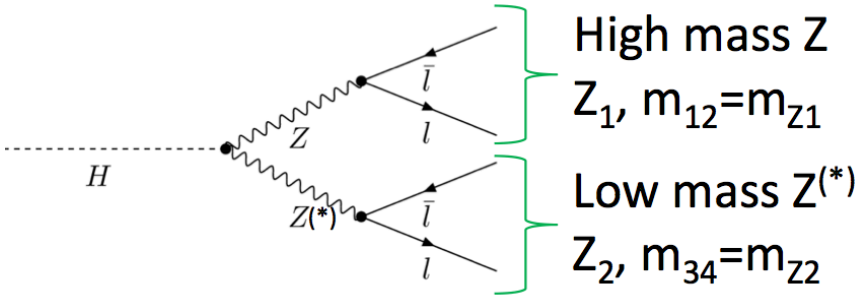

- 4 final states at low mass Higgs search: 4e, 2e2μ, 2μ2e, 4μ
- In the 2e2μ/2μ2e case, pairs ordered respect to mass

- Electrons:
  - $p_T > 7$GeV, $|\eta| < 2.47$, IP significance $< 6.5\sigma$
  - Track isolation(ΔR =0.2) < 0.15
  - Calorimeter isolation(ΔR =0.2) < 0.2
- Muons:
  - $p_T > 6$GeV, $|\eta| < 2.7$, IP significance $< 3.5\sigma$
  - Track isolation(ΔR =0.2) < 0.15
  - Calorimeter isolation(ΔR =0.2) < 0.3

H $\rightarrow$ZZ* $\rightarrow$ 4l: selections

- Final state radiation correction:
- Only for $Z_1 \rightarrow \mu\mu$:
  - 66 $< m_{12} <$89 and $m_{\mu\mu\gamma} <$ 100 GeV
- Photons :
  - $E_T <$3.5 GeV, $\Delta R <$ 0.08
  - $E_T >$3.5 GeV, $\Delta R <$ 0.15

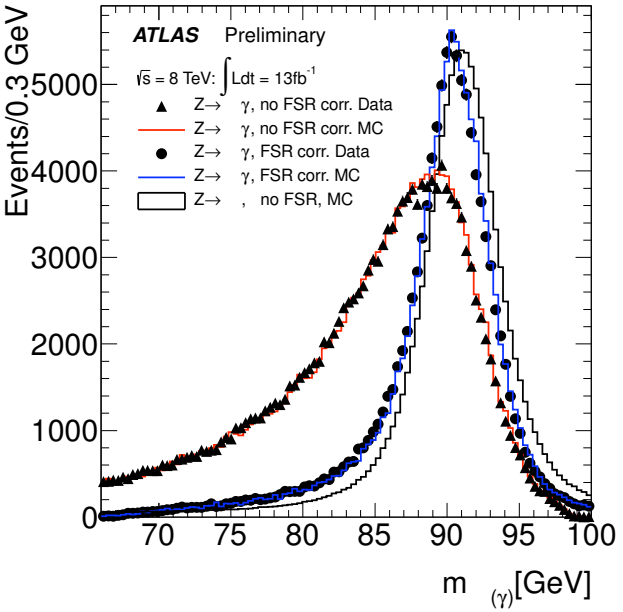

- Quadruplet:
  - $p_T >$ 20, 15, 10, 7 GeV ($>$ 6 GeV if the 4th lepton is a muon)
  - m_{12} = [50, 106] GeV, m_{34} = [12*, 115] GeV
    - *Lower cut increase for $m_{4l} >$140 GeV
- Signal selection efficiencies:
  - 39% for 4μ, 26% for 2e2μ/2μ2e and 19% for 4e channel

H $\rightarrow$ZZ* $\rightarrow$ 4l: signal mass resolution

4e: 2.0σ

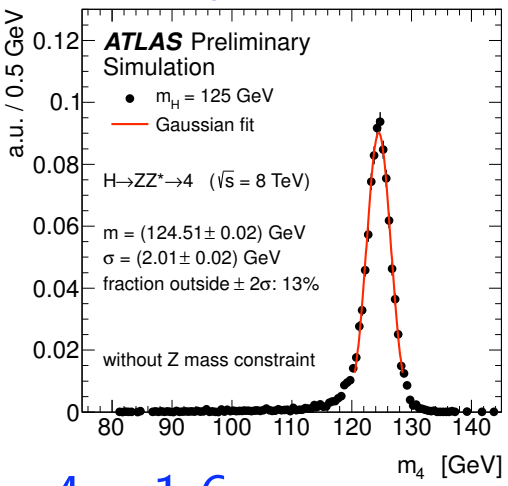

2e2μ/2μ2e: 2.3σ

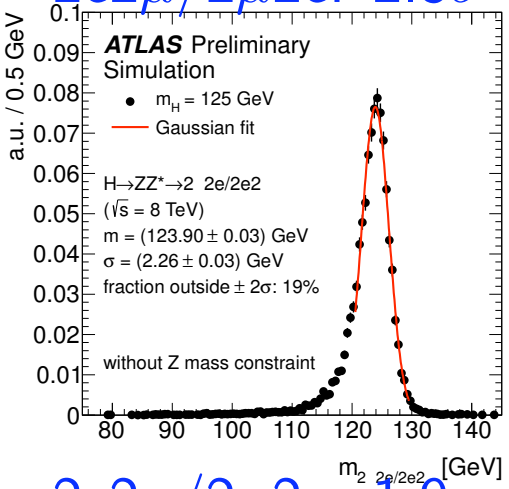

4μ: 2.7σ

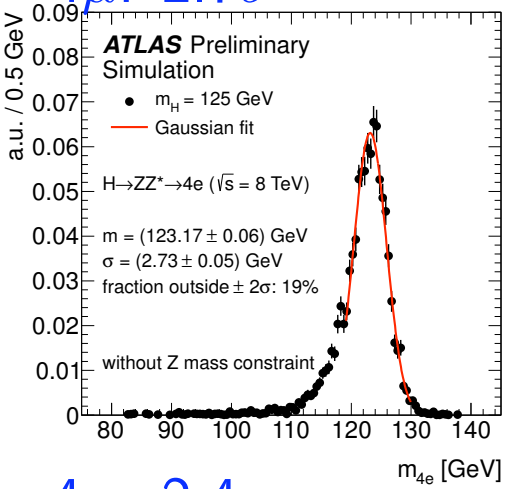

4e: 1.6σ

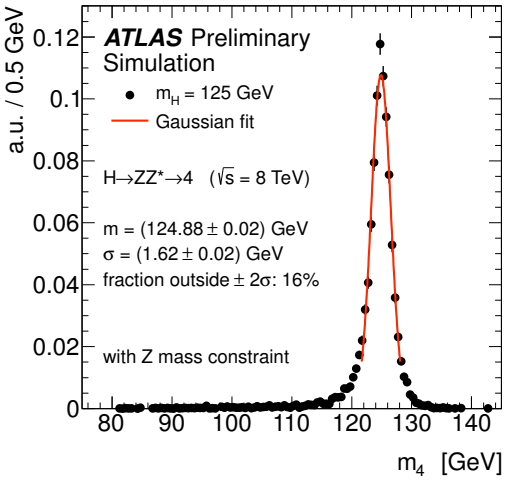

2e2μ/2μ2e: 1.9σ

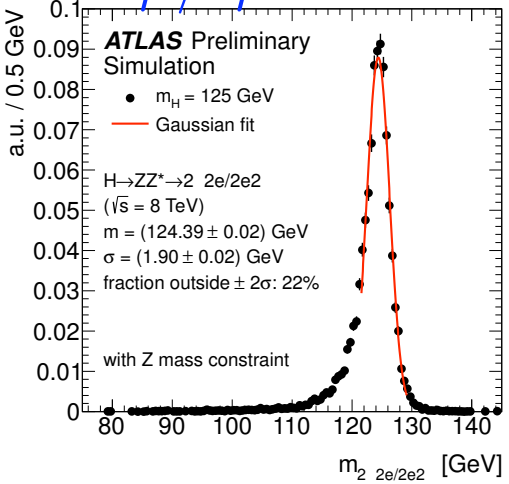

4μ: 2.4σ

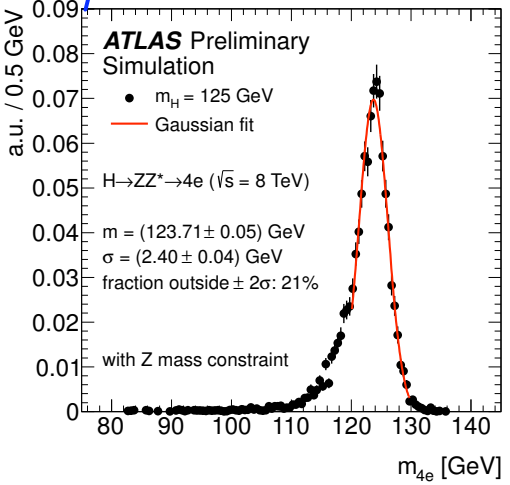

H $\rightarrow$ZZ* $\rightarrow$ 4l: backgrounds

- ZZ* di-boson production: irreductible background
  - Estimated using MC simulation normalized to the theoretical cross section.
- Z+jets, ttbar: reducible background
- Estimated with data]driven methods with Z+ll and Z+l control regions
  - Increase the statistics by loosening or inverting the selections of additional lepton(s)
  - Estimate background composition
  - Extrapolate the background composition to the signal region based on simulation

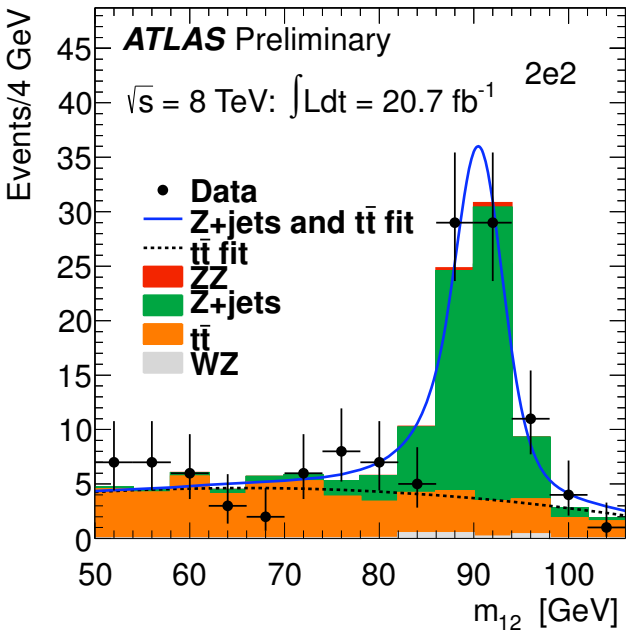

H →ZZ* → 4l: backgrounds

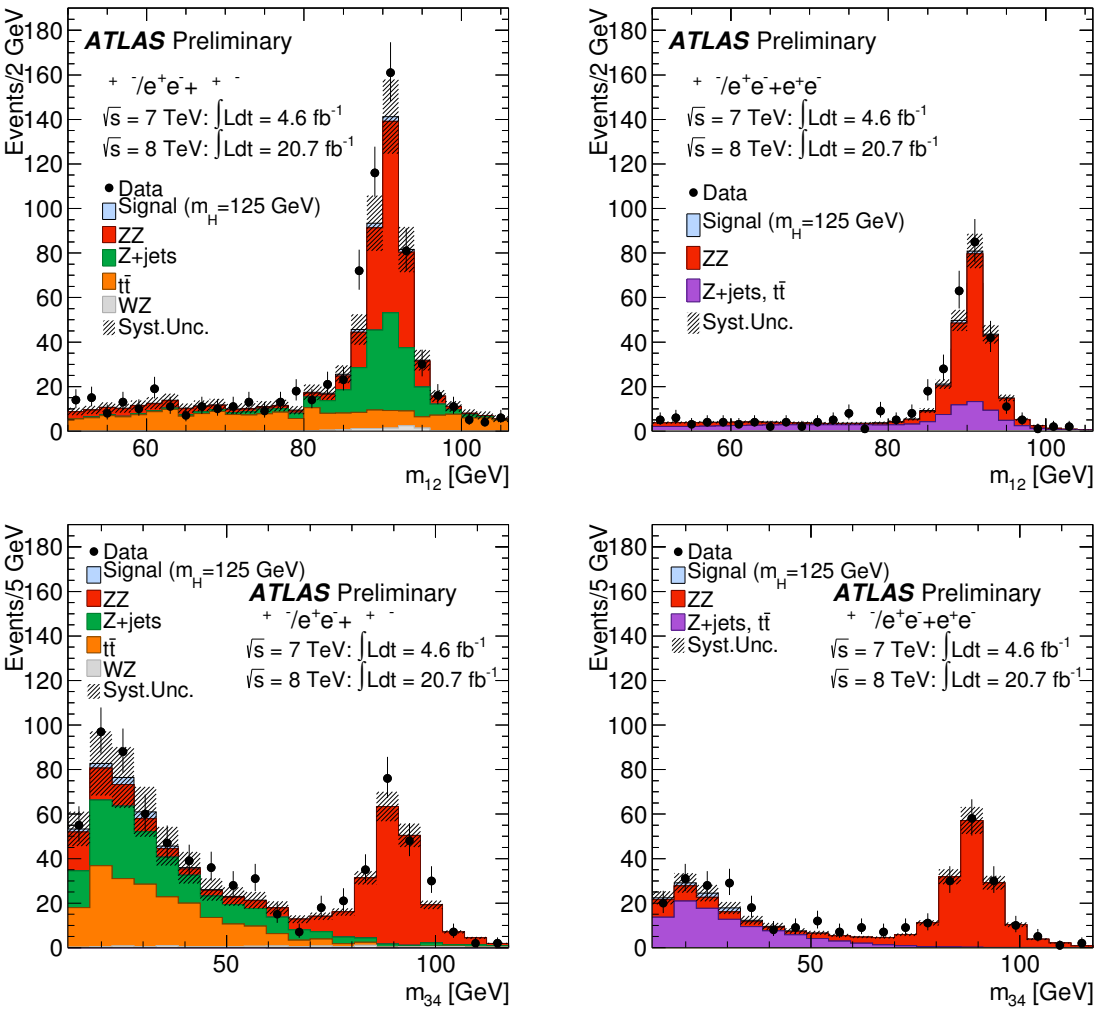

- The MC is normalised to the data-driven background estimations
- Good agreements between data and MC

H $\rightarrow$ZZ* $\rightarrow$ 4l: categorization

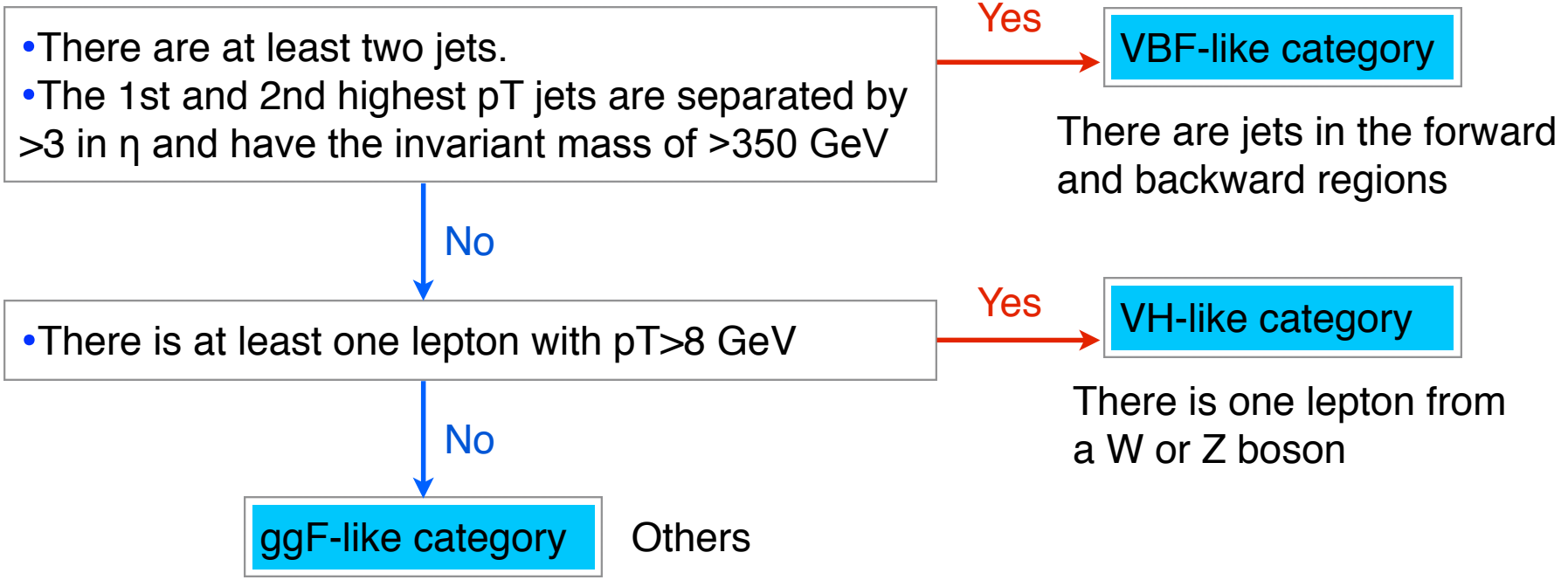

H $\rightarrow$ZZ* $\rightarrow$ 4l: categorization

category	$gg \to H, q\bar{q}/gg \to t\bar{t}H$	$qq' \to Hqq'$	$q\bar{q} \to W/ZH$	$ZZ^{(*)}$
		$\sqrt{s} = 8\,\text{TeV}$		
ggF-like	13.5	0.79	0.65	320.4
VBF-like	0.28	0.43	0.01	3.58
VH-like	0.06	-	0.14	0.69
		$\sqrt{s} = 7\,\text{TeV}$		
ggF-like	2.20	0.14	0.11	57.5
VBF-like	0.03	0.06	-	0.44
VH-like	0.01	-	0.03	0.25

H $\rightarrow$ZZ* $\rightarrow$ 4l: systematic uncertainties

- **Mass measurement**
- Decay modes involving electrons (4e, 2e2μ): electron energy scale uncertainty is main contributor
  - 0.4% (0.2%) on measured mass in 4e (2e2μ)
- Decay modes involving muons (4μ, 2μ2e): muon momentum scale, resolution uncertainty are main contributors
  - 0.2% (0.1%) on measured mass in 4μ (2μ2e)
- **Signal strength measurement**
- Decay modes involving electrons: electron ID and reco efficiency
  - 9.4% in 4e, 8.7% in 2e2μ, 2.4% in 2μ2e
- Decay modes involving muons: muon ID and reco efficiency
  - 0.8% in 4e, 8.7% in 2e2μ, 2.4% in 2μ2e

H →ZZ* → 4l: results

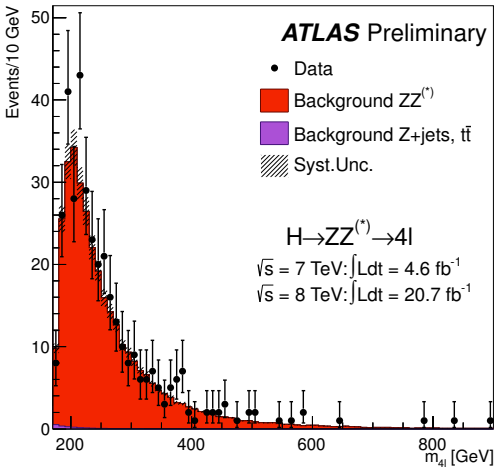

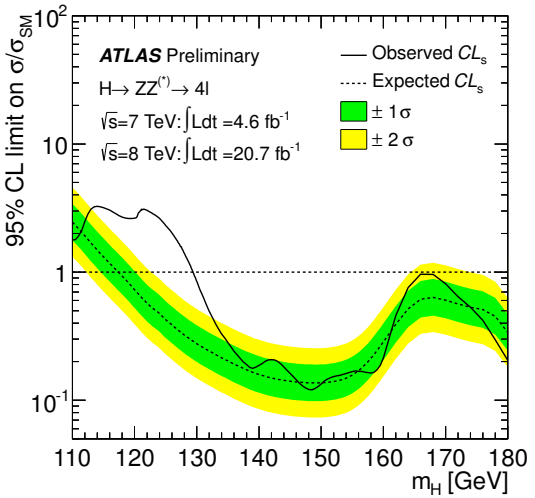

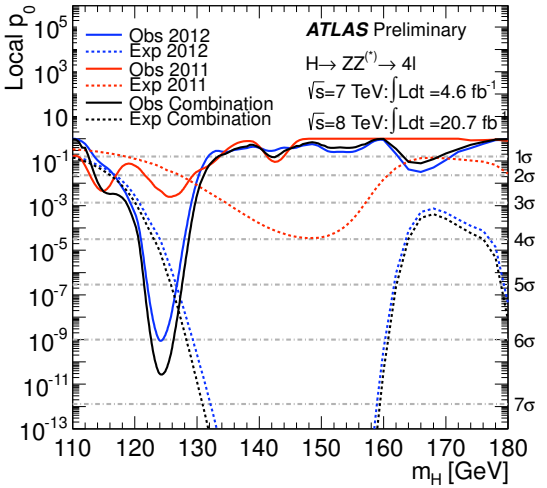

Table 8: Summary of the observed and expected p_0-values for the $\sqrt{s} = 7\,\text{TeV}$, $\sqrt{s} = 8\,\text{TeV}$ data sets and their combination. The expected p_0-value is quoted at the mass of the observed minimum.

	observed			expected	
data set	min p_0	significance $[\sigma]$	$m_H(p_0)$	min $p_0(m_H)$	significance $[\sigma]$
$\sqrt{s} = 7\,\text{TeV}$	2.5×10^{-3}	2.8	125.6 GeV	3.5×10^{-2}	1.8
$\sqrt{s} = 8\,\text{TeV}$	8.8×10^{-10}	6.0	124.1 GeV	2.8×10^{-5}	4.0
combined	2.7×10^{-11}	6.6	124.3 GeV	5.7×10^{-6}	4.4

H →ZZ* → 4l: results

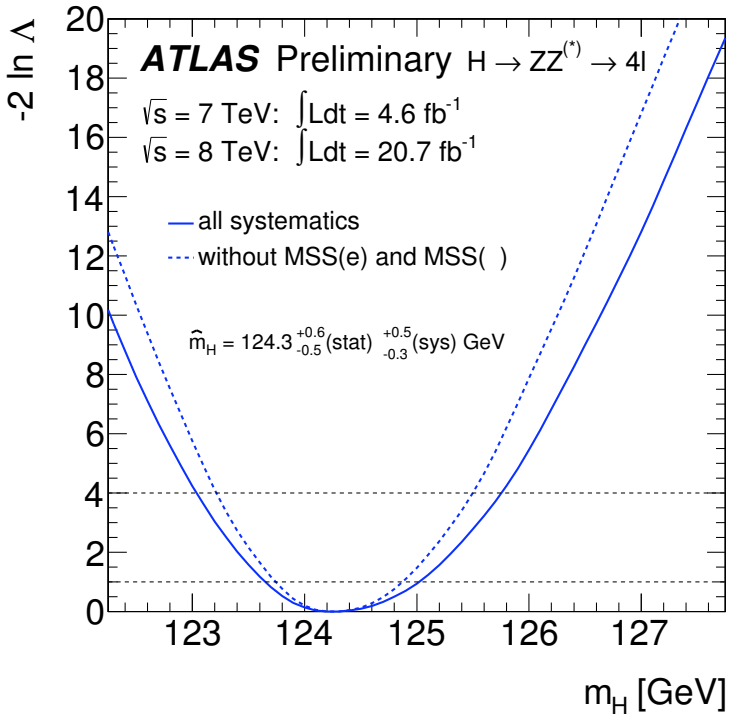

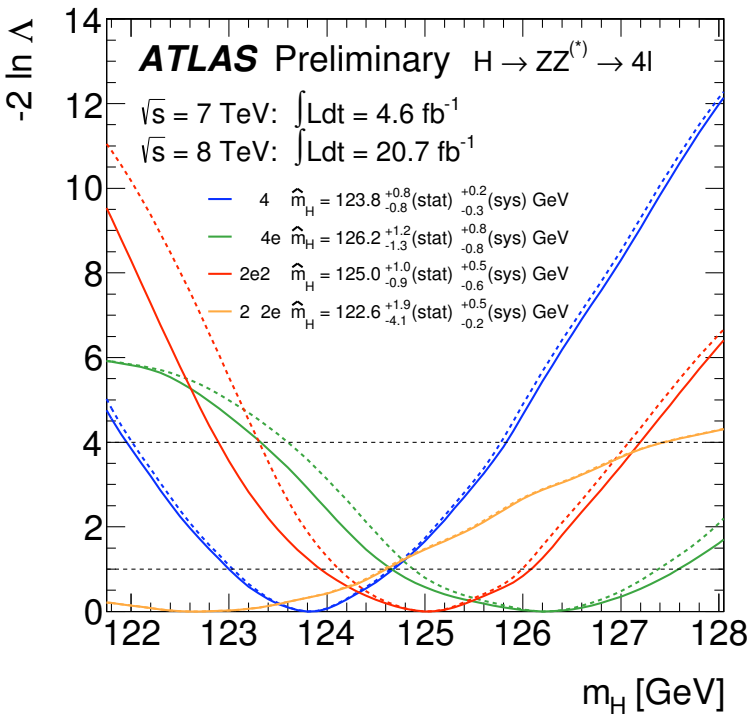

- The profile likelihood as a function of m_H

H →ZZ* → 4l: spin

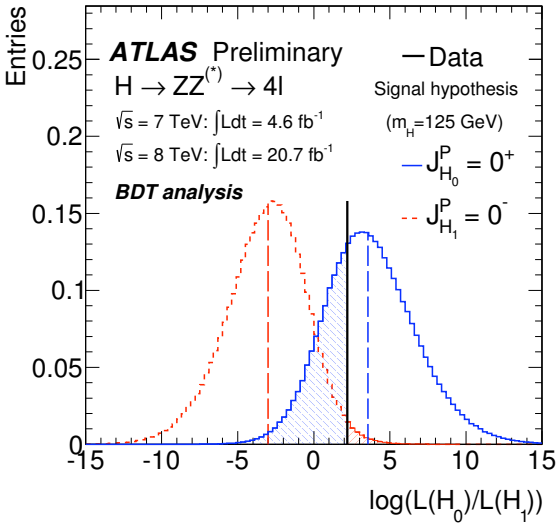
ATLAS Preliminary
H → ZZ(*) → 4l
√s = 7 TeV: ∫Ldt = 4.6 fb-1
√s = 8 TeV: ∫Ldt = 4.6 fb-1
BDT analysis
Data
Signal hypothesis
(mH=125 GeV)
JPH0 = 0+
JPH1 = 0-
Entries
log(L(H0)/L(H1))

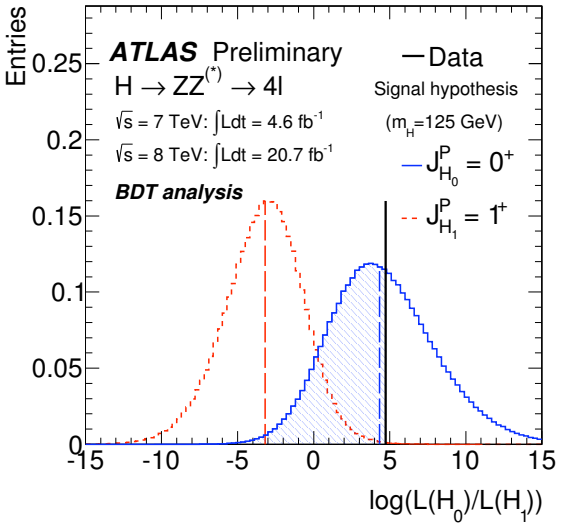
ATLAS Preliminary
H → ZZ(*) → 4l
√s = 7 TeV: ∫Ldt = 4.6 fb-1
√s = 8 TeV: ∫Ldt = 4.6 fb-1
BDT analysis
Data
Signal hypothesis
(mH=125 GeV)
JPH0 = 0+
JPH1 = 1+
Entries
log(L(H0)/L(H1))

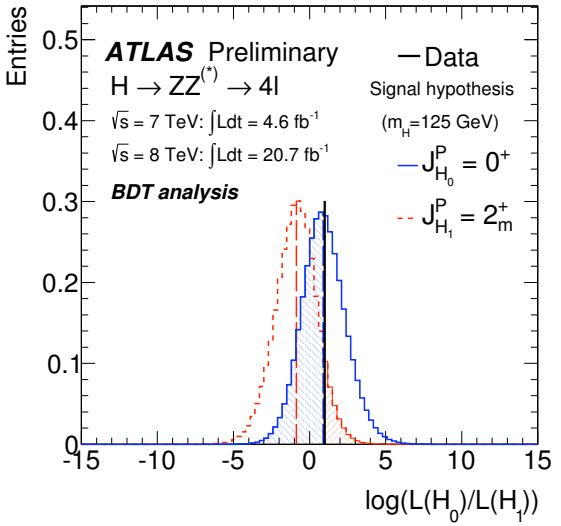
ATLAS Preliminary
H → ZZ(*) → 4l
√s = 7 TeV: ∫Ldt = 4.6 fb-1
√s = 8 TeV: ∫Ldt = 4.6 fb-1
BDT analysis
Data
Signal hypothesis
(mH=125 GeV)
JPH0 = 0+
JPH1 = 2+m
Entries
log(L(H0)/L(H1))

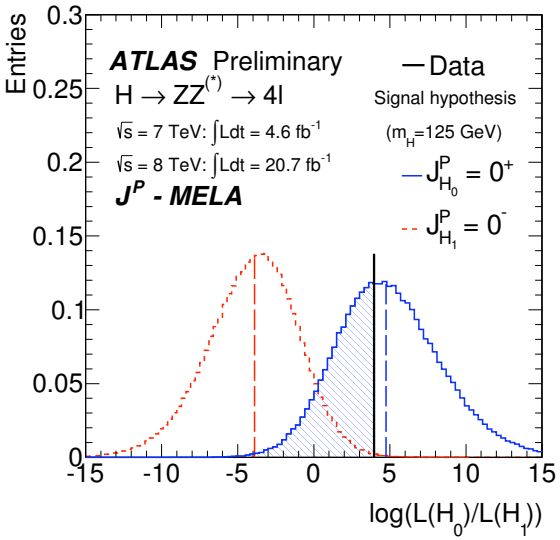
ATLAS Preliminary
H → ZZ(*) → 4l
√s = 7 TeV: ∫Ldt = 4.6 fb-1
√s = 8 TeV: ∫Ldt = 4.6 fb-1
JP - MELA
Data
Signal hypothesis
(mH=125 GeV)
JPH0 = 0+
JPH1 = 0-
Entries
log(L(H0)/L(H1))

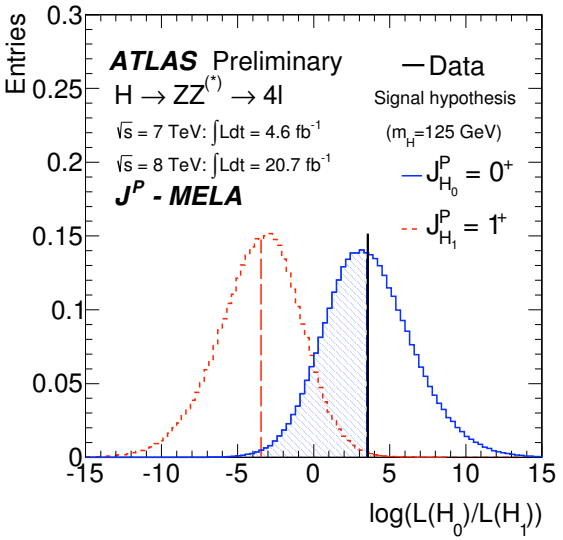
ATLAS Preliminary
H → ZZ(*) → 4l
√s = 7 TeV: ∫Ldt = 4.6 fb-1
√s = 8 TeV: ∫Ldt = 4.6 fb-1
JP - MELA
Data
Signal hypothesis
(mH=125 GeV)
JPH0 = 0+
JPH1 = 1+
Entries
log(L(H0)/L(H1))

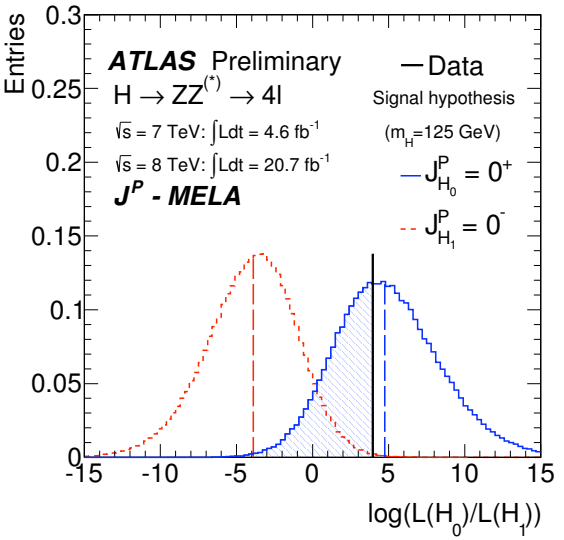
ATLAS Preliminary
H → ZZ(*) → 4l
√s = 7 TeV: ∫Ldt = 4.6 fb-1
√s = 8 TeV: ∫Ldt = 4.6 fb-1
JP - MELA
Data
Signal hypothesis
(mH=125 GeV)
JPH0 = 0+
JPH1 = 0-
Entries
log(L(H0)/L(H1))

H $\rightarrow$WW* $\rightarrow$ lvlv: selections

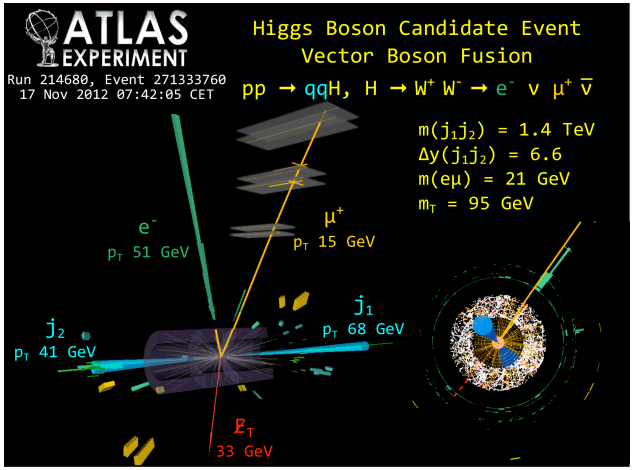

- Analysis performed in 4-channels:
  - Different flavor: eμ, μe
  - Same flavor: ee, $\mu\mu$
- Split by jet-multiplicity: $0/1/\geq 2$
- Discriminating variables:
  - $p_{T,ll}$, m_{ll}, $\Delta\Phi_{ll}$, m_T

- Leptons:
  - Exact two leptons. $p_T > 25, 15$ GeV
- Missing E_T, charged track MET:
  - Relative to leptons and jets. Track MET only in same flavor channel
  - MET rel $>$ 25 GeV(DF), $>$ 45 GeV(SF)
  - Track MET rel $>$ 45 GeV(SF)

H $\rightarrow$WW* $\rightarrow$ lvlv: selections

- Topological selections:
  - m_{ll} >10 GeV(DF), > 12 GeV(SF)
  - $m_{ll} < 50$ GeV($N_{jet} = 0, 1$), < 60 GeV($N_{jet} \geq 2$)
  - $\Delta\Phi < 1.8$
  - $93.45 < m_T < 125$ GeV for $N_{jet} = 0, 1$. $m_T < 150$ GeV for $N_{jet} \geq 2$
- Z$\rightarrow \tau\tau$ veto for $N_{jet} = 1, \geq 2$

Number of jets

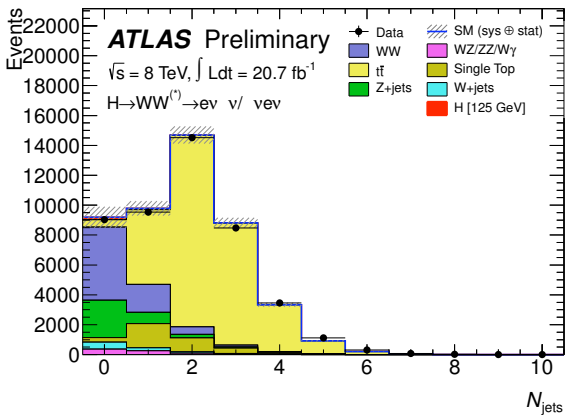

MET rel

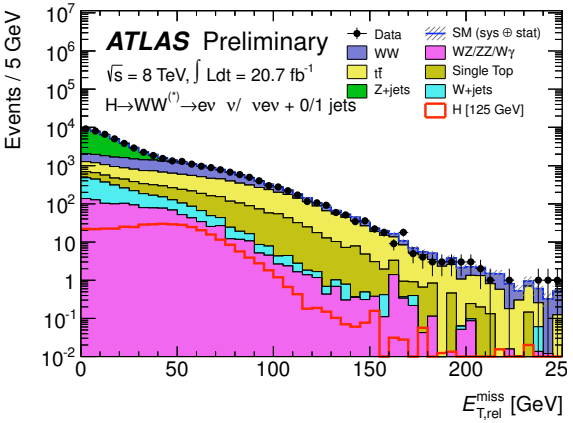

m_{ll}

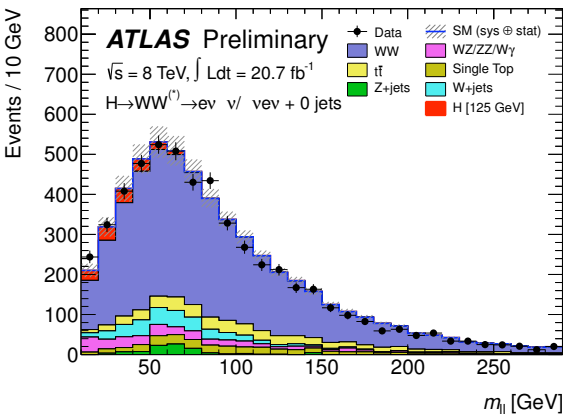

H $\rightarrow$WW* $\rightarrow$ lvlv: backgrounds

- **W+jets** : C.R + "fake factor"

Estimated W+jets background

$$N_{\text{one id(from W)+one fake}} = \frac{N_{\text{id obj}}}{N_{\text{anti-id obj}}} \times N_{\text{one id(fromW)+one anti-id}}$$

W+jets control region to determine normalization (Observable)

Fake factor(Observable)

- **WW** and **Top** : MC prediction is normalized using data C.R.
- **Z+jets** : Z-> $\tau\tau$ C.R, f_{recoil}
- **Di-bosons(WZ/Wγ^*/Wγ** and **ZZ**) : using MC.

WW C.R

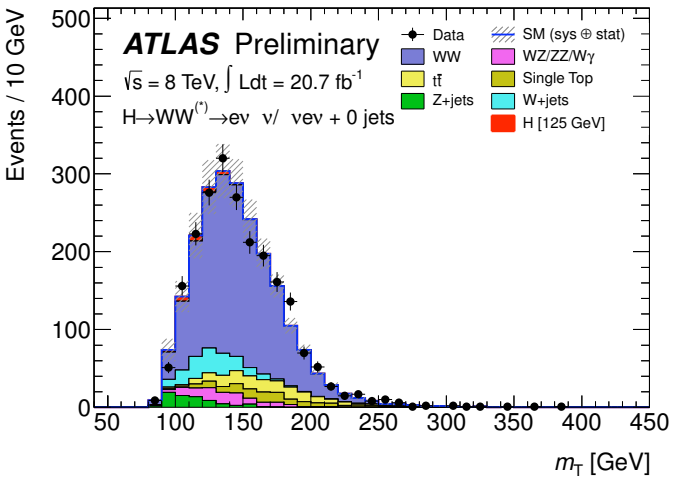

H $\rightarrow$WW* $\rightarrow$ lvlv: m_T

0 ets

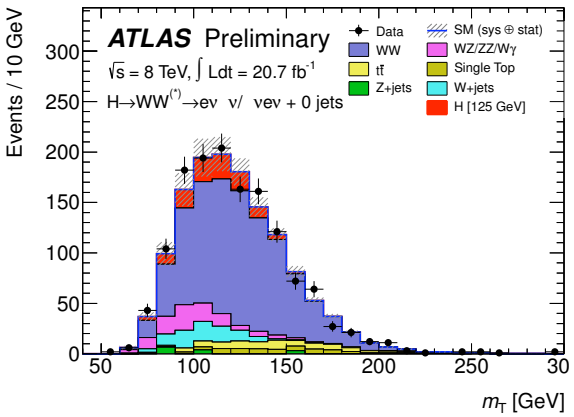

1 jet

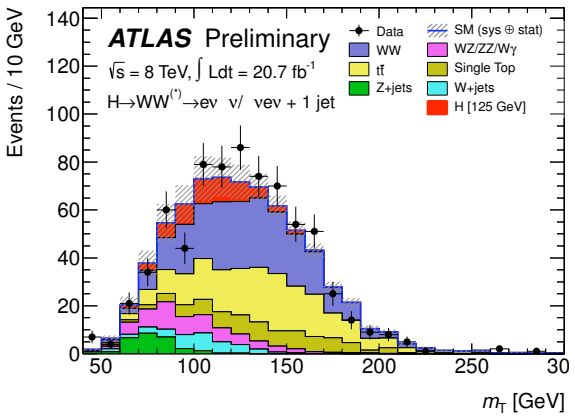

$\geq$2 jet

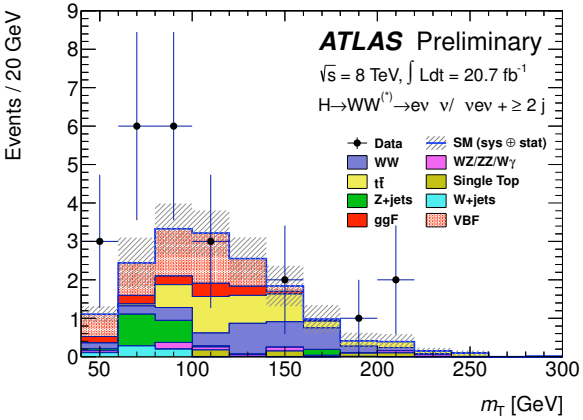

- Different flavor results are shown
- Data well agree with the expectation including 125 GeV Higgs signals

H $\rightarrow$WW* $\rightarrow$ lvlv: systematic uncertainties

Table 13: Leading uncertainties on the signal strength μ for the combined 7 and 8 TeV analysis.

Category	Source	Uncertainty, up (%)	Uncertainty, down (%)
Statistical	Observed data	+21	−21
Theoretical	Signal yield ($\sigma \cdot \mathcal{B}$)	+12	−9
Theoretical	WW normalisation	+12	−12
Experimental	Objects and DY estimation	+9	−8
Theoretical	Signal acceptance	+9	−7
Experimental	MC statistics	+7	−7
Experimental	W+ jets fake factor	+5	−5
Theoretical	Backgrounds, excluding WW	+5	−4
Luminosity	Integrated luminosity	+4	−4
Total		+32	−29

H →WW* → lνlν: results

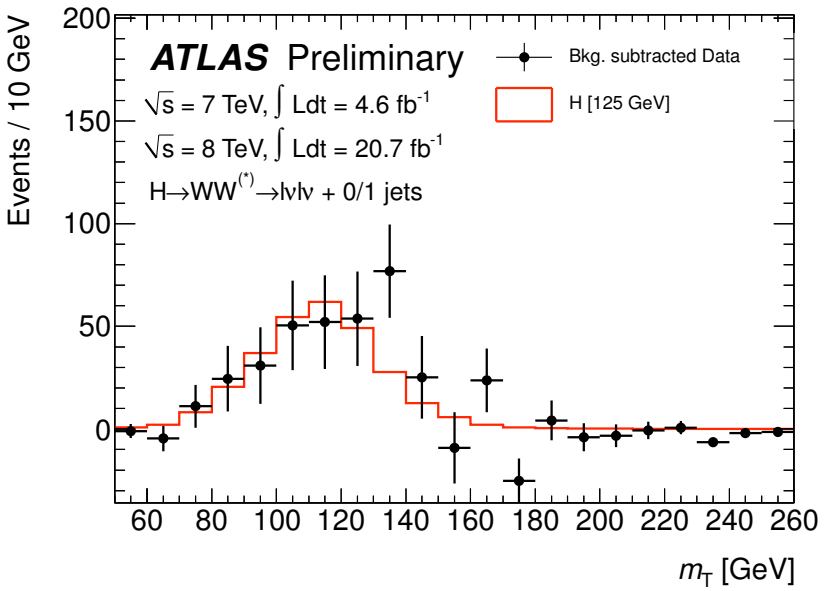

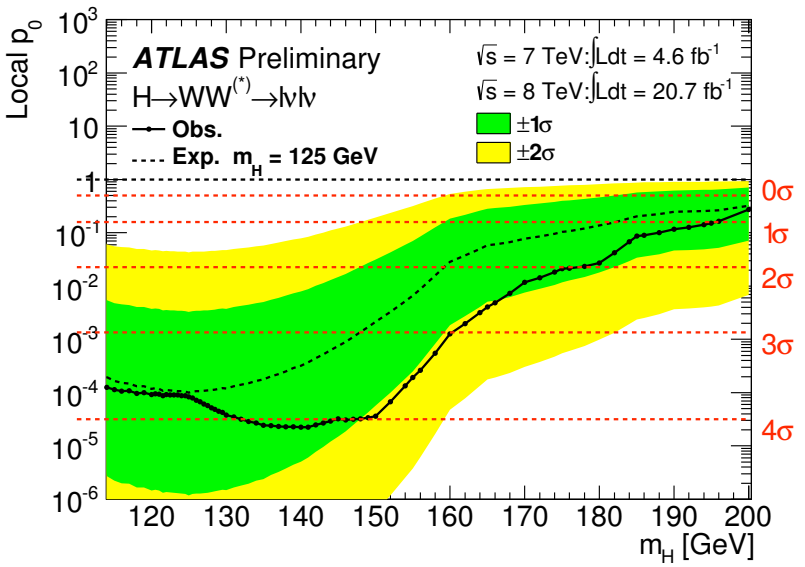

- An excess of events over the expected background is observed for $m_H < 150$ GeV with the largest significance of 4.1 standard deviations (p0 $= 2\times10^{-5}$) at $m_H = 140$ GeV
- The signal significance at $m_H = 125$ GeV is 3.8 standard deviations (p0 $= 8\times10^{-5}$)

H →WW* → lνlν: spin

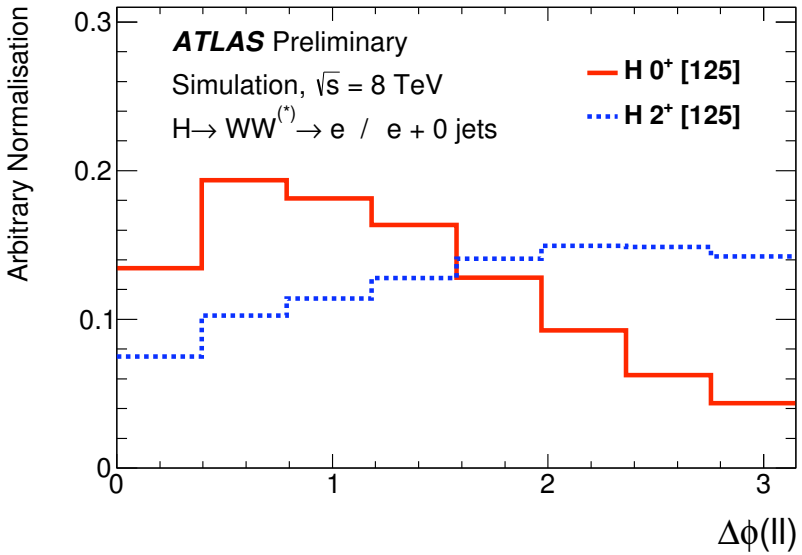

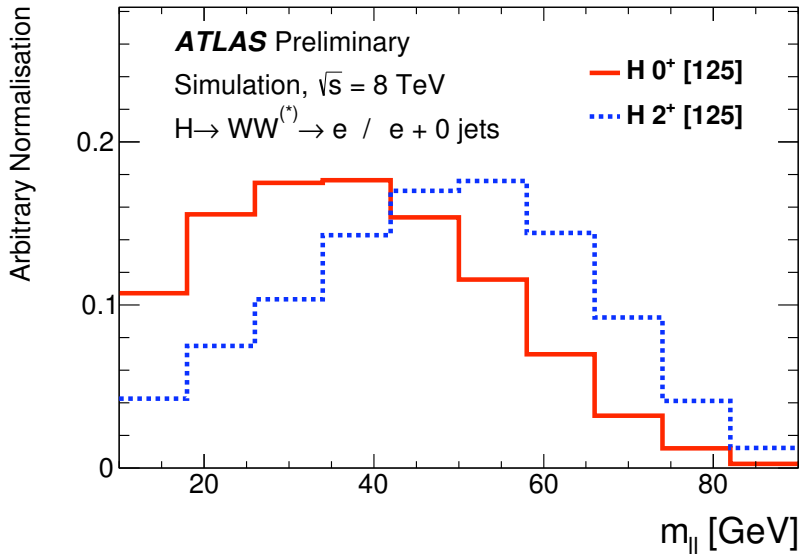

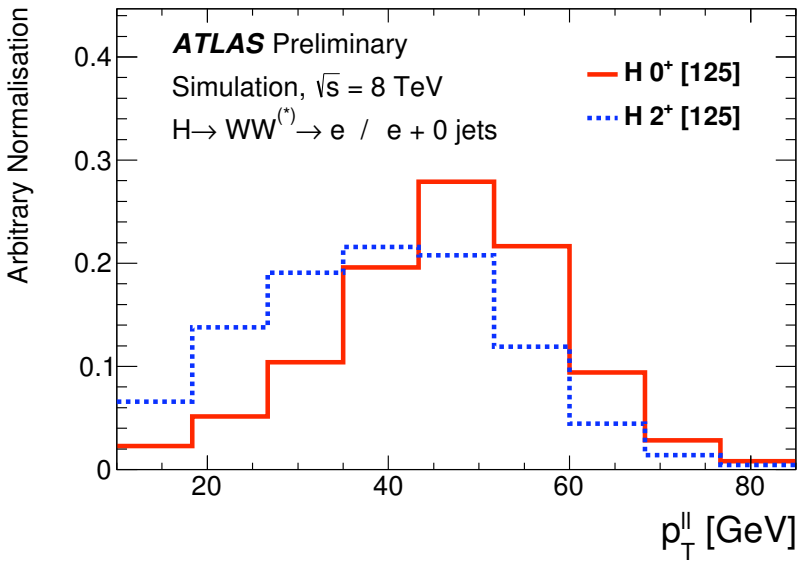

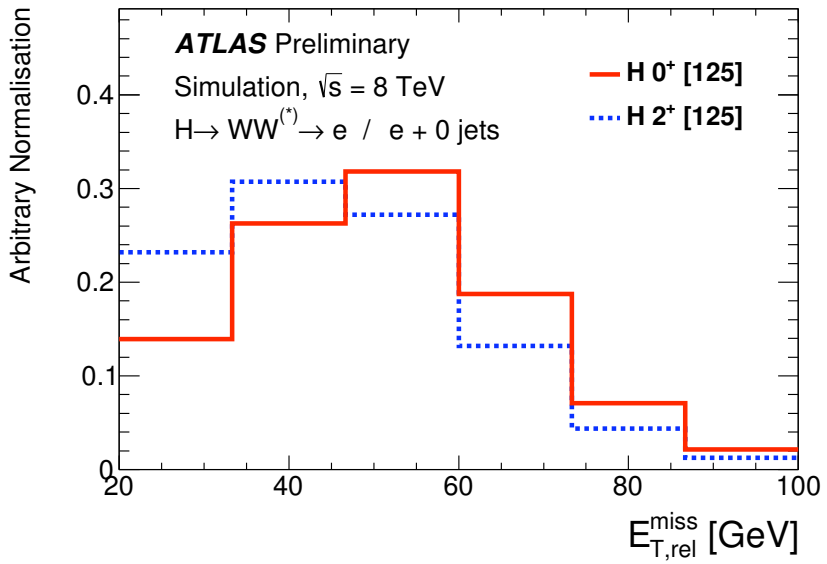

H →WW* → lνlν: spin

- BDT output distributions in the signal region

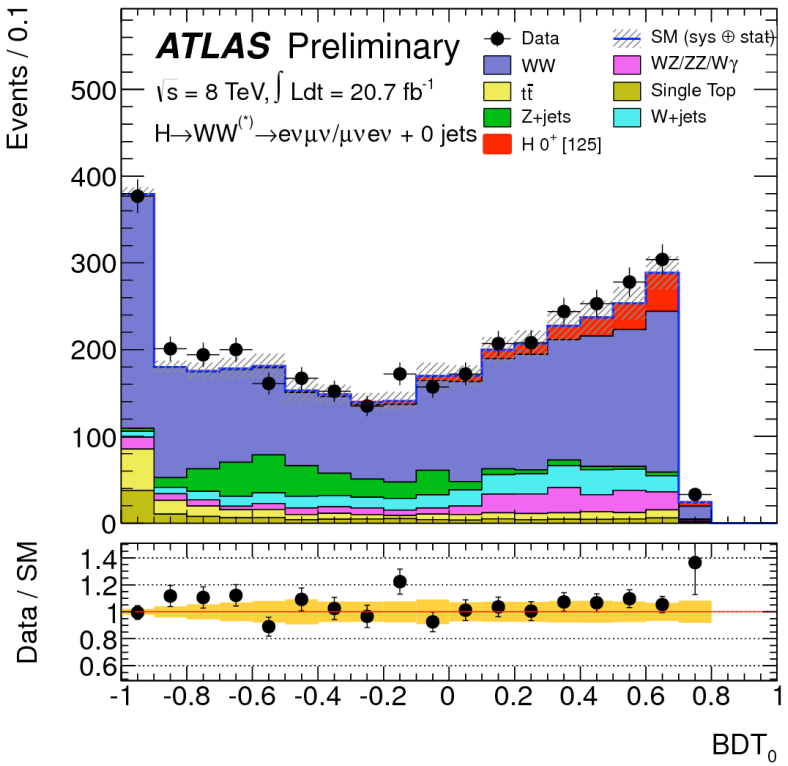

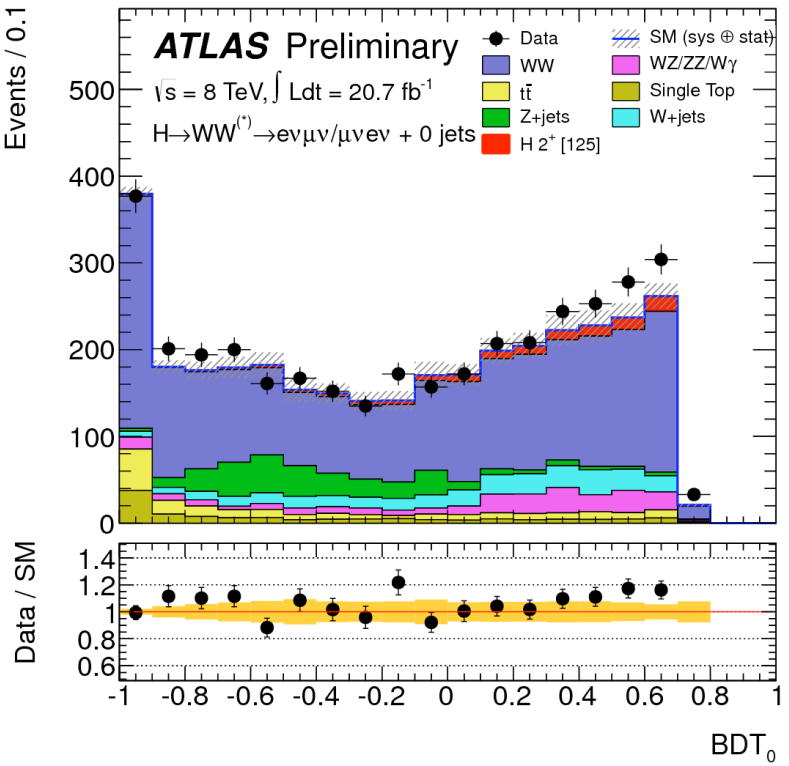

H →WW* → lνlν: spin

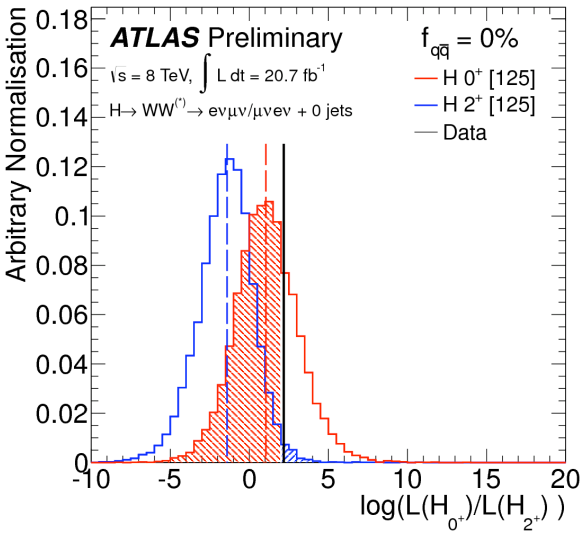

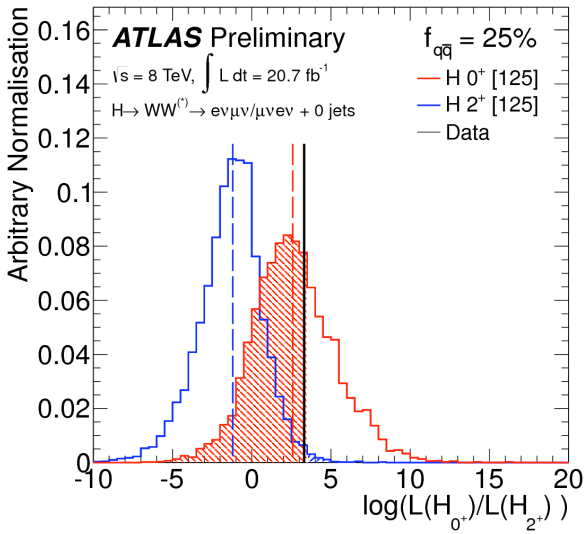

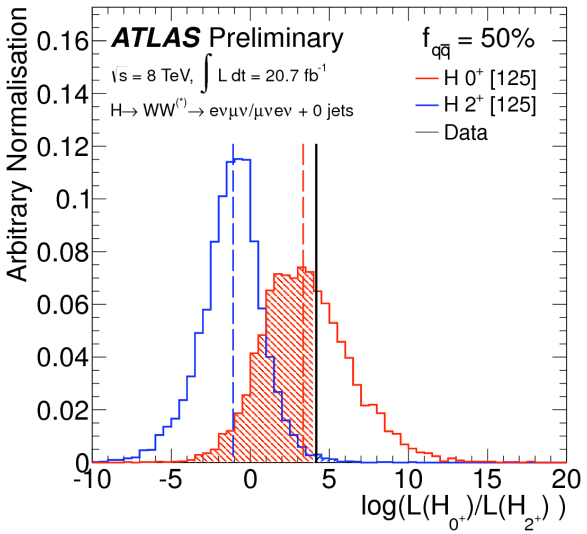

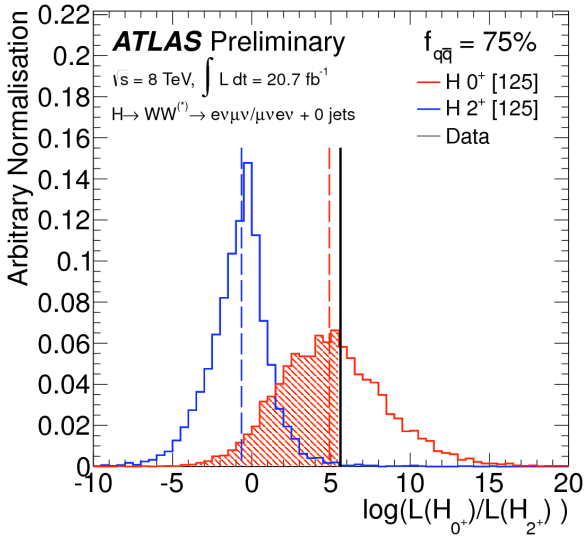

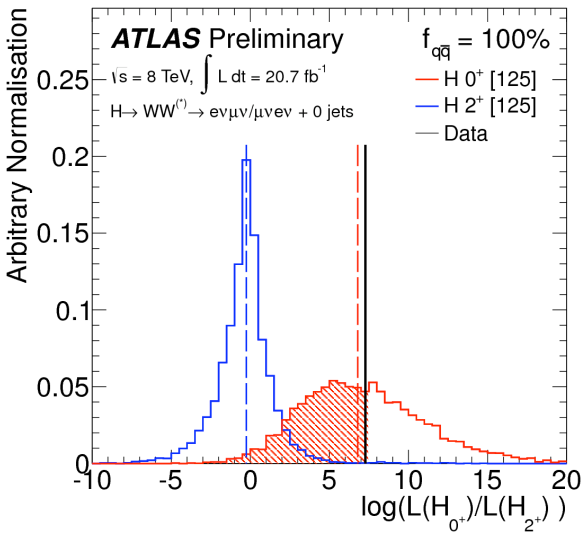

H $\rightarrow$Zγ $\rightarrow$ llγ: selections

- The Higgs boson decays to Zγ via loop diagrams similar to H $\rightarrow \gamma\gamma$

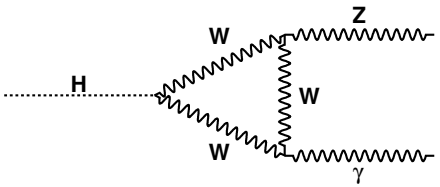

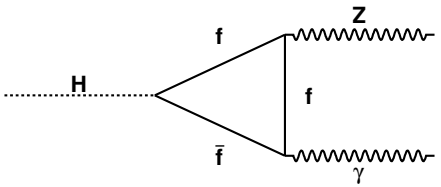

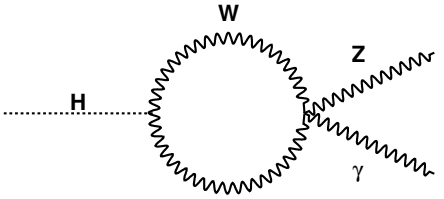

- 2 (same flavor and opposite sign) isolated leptons, p_T >10 GeV and $m_{ll} > m_Z$ - 10 GeV
- 1 isolated photon, E_T >15 GeV and $\Delta R_{l\gamma} > 0.3$

H $\rightarrow$Zγ $\rightarrow$ llγ: backgrounds

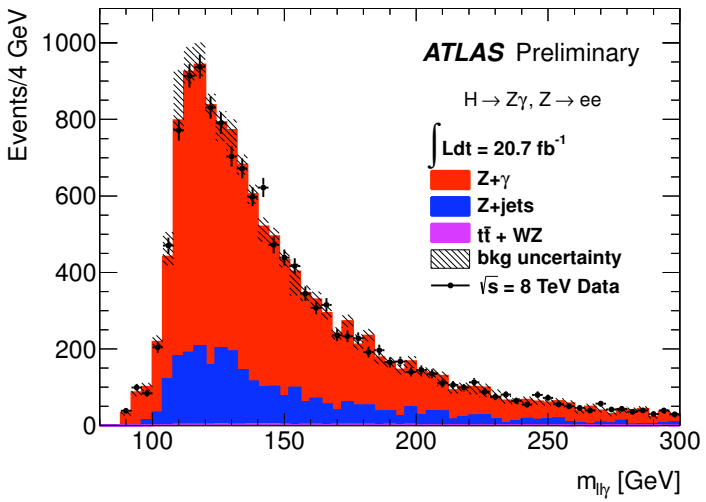

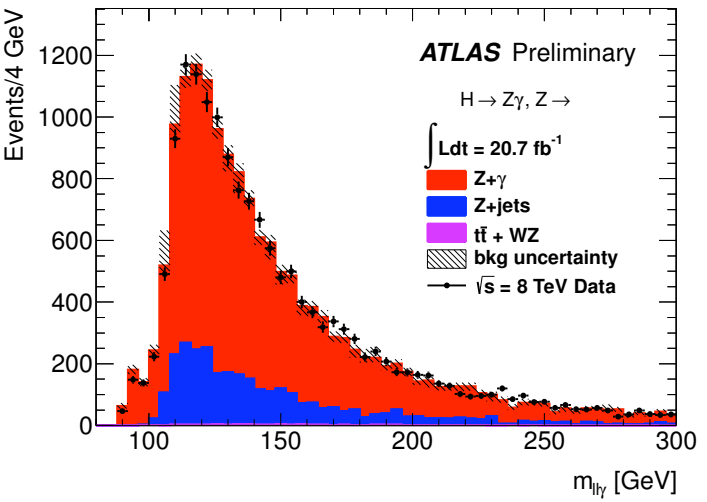

- Use MC to estimate $t\bar{t}$ + WZ backgrounds
- Data-driven background decomposition (photon ID vs isolation) after subtraction of $t\bar{t}$ + WZ to disentangle Z+γ from Z+j

H →Zγ → llγ: results

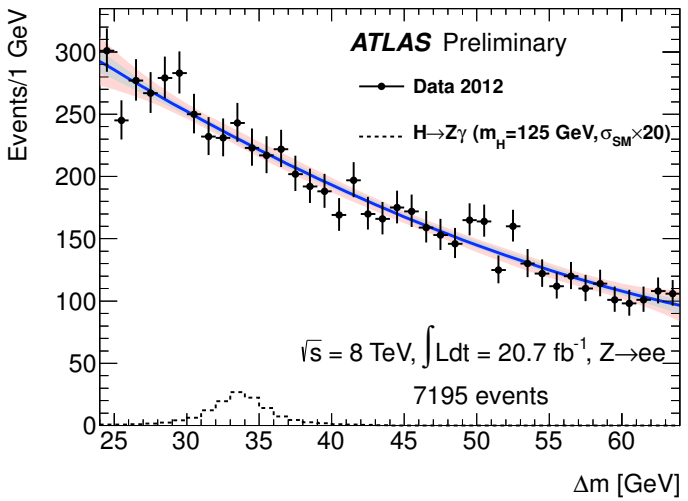

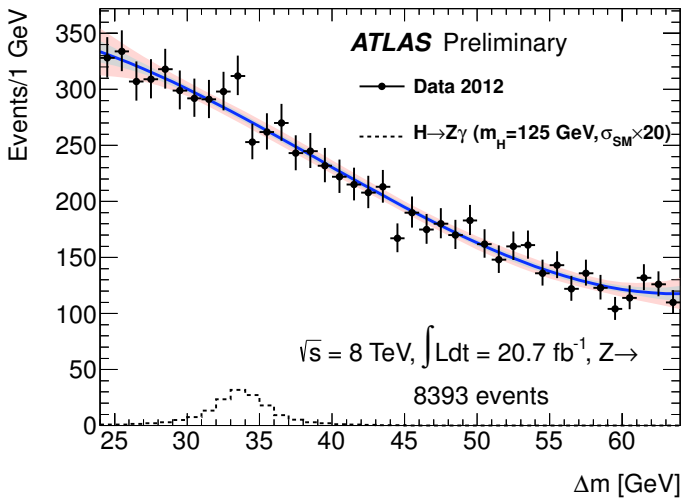

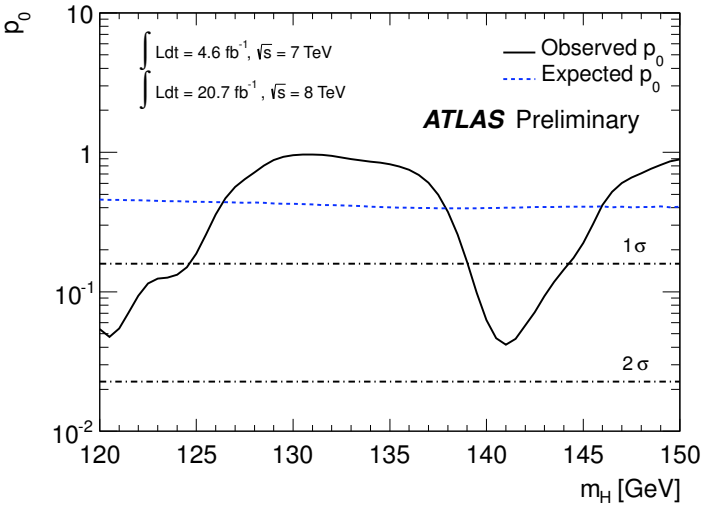

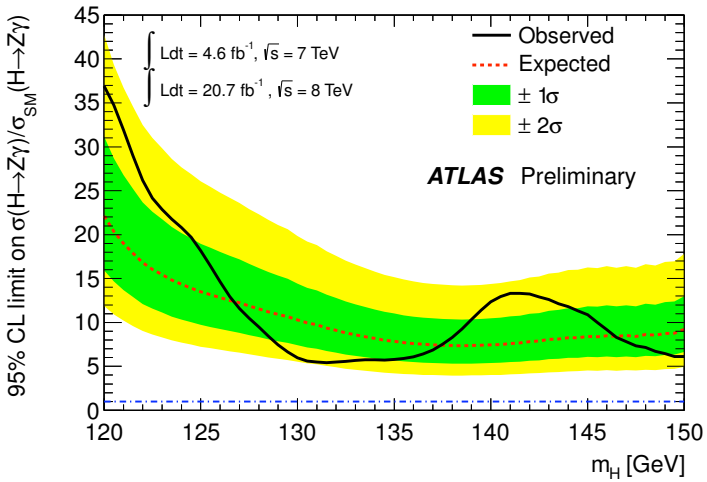

MELA

- $J^P - MELA$ discriminant defined as:

$$J^P - MELA = \frac{P(H_0)}{P(H_0)+P(H_1)}$$

- $P(H_0) \rightarrow$ probability density function of H_i hypothesis including detector/selection effects
- Compute exact probability for a spin-CP state for each event
- Detector acceptance cancels in the ratio